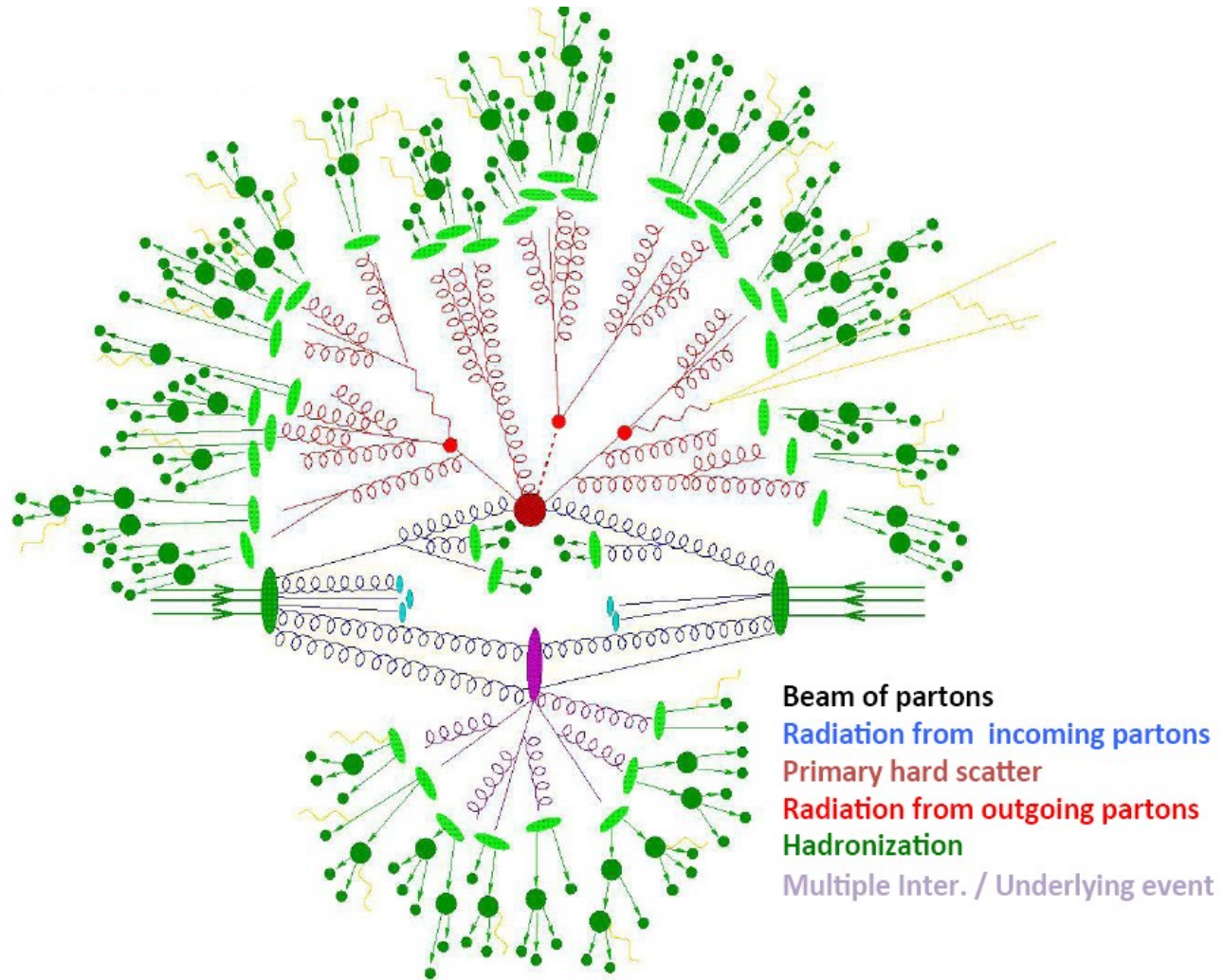


Physics Program of the experiments at Large Hadron Collider

- **Hard QCD**
 - **More on structure functions from HERA**
 - **Constraints from recent ATLAS results**

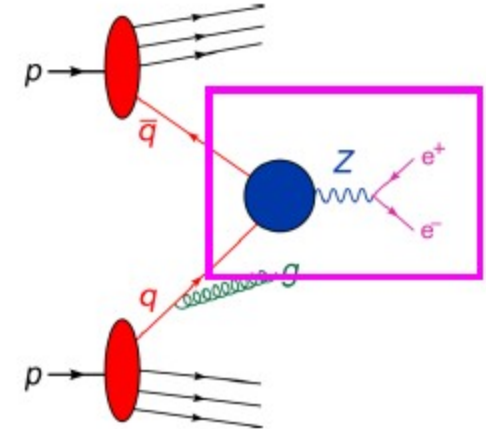


Typical pp collision



QCD factorisation and parton model

- Asymptotic freedom guarantees that at short distances (large transverse momenta) partons in the proton are almost free
- Sampled "one at a time" in hard collisions
 - QCD improved parton shower model



“suitable” final state

Parton distribution function:
prob. of finding parton a in proton 1,
carrying fraction x_1 of its momentum

factorization scale (“arbitrary”)

$$\sigma^{pp \rightarrow X}(s; \alpha_s, \mu_R, \mu_F) = \sum_{a,b} \int_0^1 dx_1 \int_0^1 dx_2 f_a(x_1, \alpha_s, \mu_F) f_b(x_2, \alpha_s, \mu_F) \times \hat{\sigma}^{ab \rightarrow X}(sx_1x_2; \alpha_s, \mu_R, \mu_F)$$

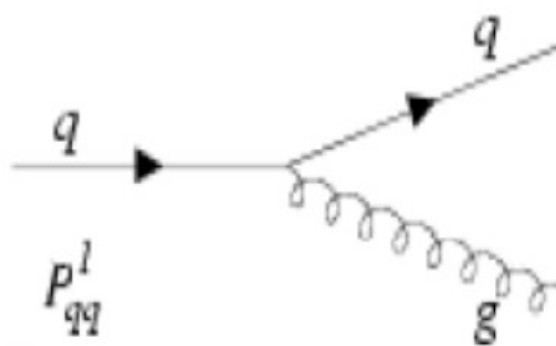
Partonic cross section,
computable in perturbative QCD

partonic CM energy²

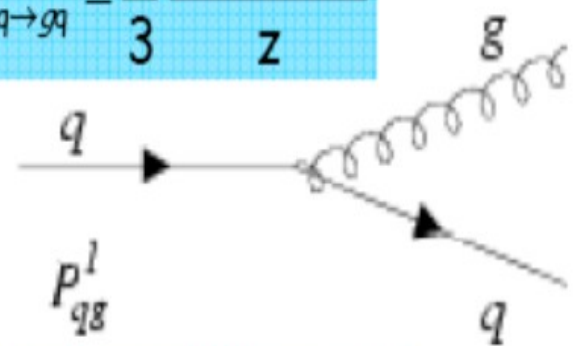
renormalization scale (“arbitrary”)

Altarelli-Parisi splitting functions

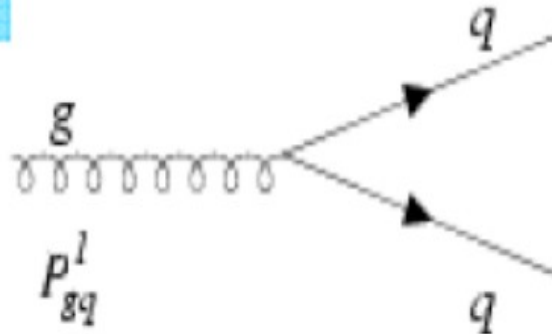
$$P_{q \rightarrow qg}^l = \frac{4}{3} \left(\frac{1+z^2}{1-z} \right)$$



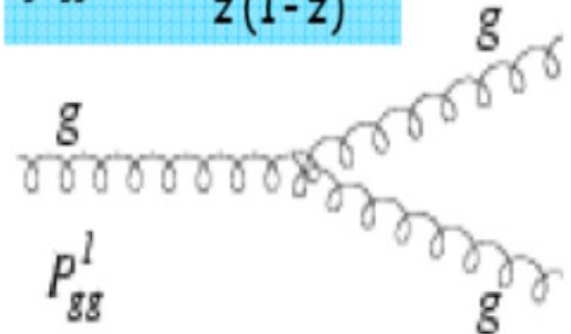
$$P_{q \rightarrow gq}^l = \frac{4}{3} \frac{1+(1-z)^2}{z}$$



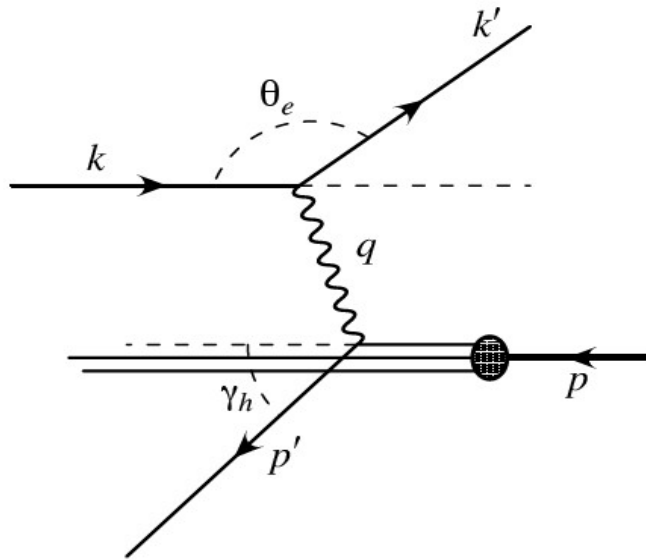
$$P_{g \rightarrow qq}^l = \frac{n_f^2}{2} (z^2 + (1-z)^2)$$



$$P_{g \rightarrow gg}^l = 3 \frac{(1-z)(1-z)^2}{z(1-z)}$$



Deep Inelastic Scattering



Momentum transfer :

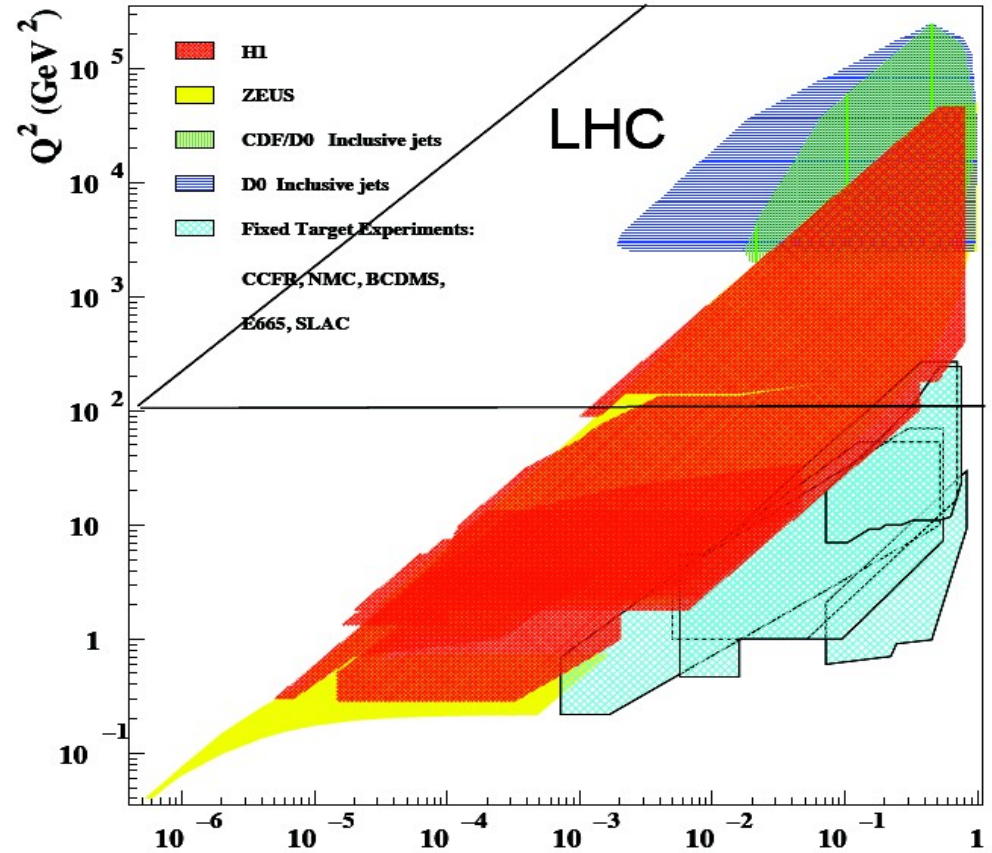
$$Q^2 = -q^2 = -(k-k')^2$$

Momentum fraction carried by struck parton :

$$x = Q^2/(2p \cdot q)$$

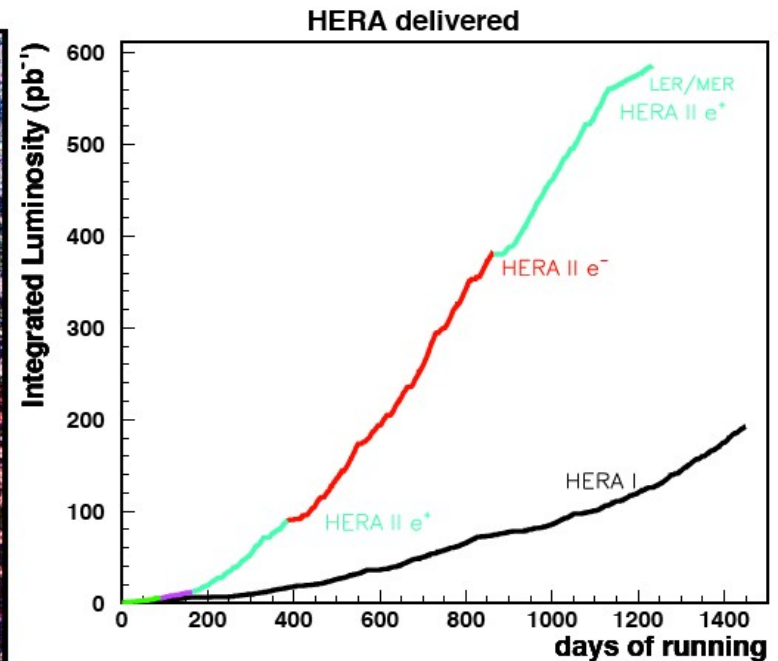
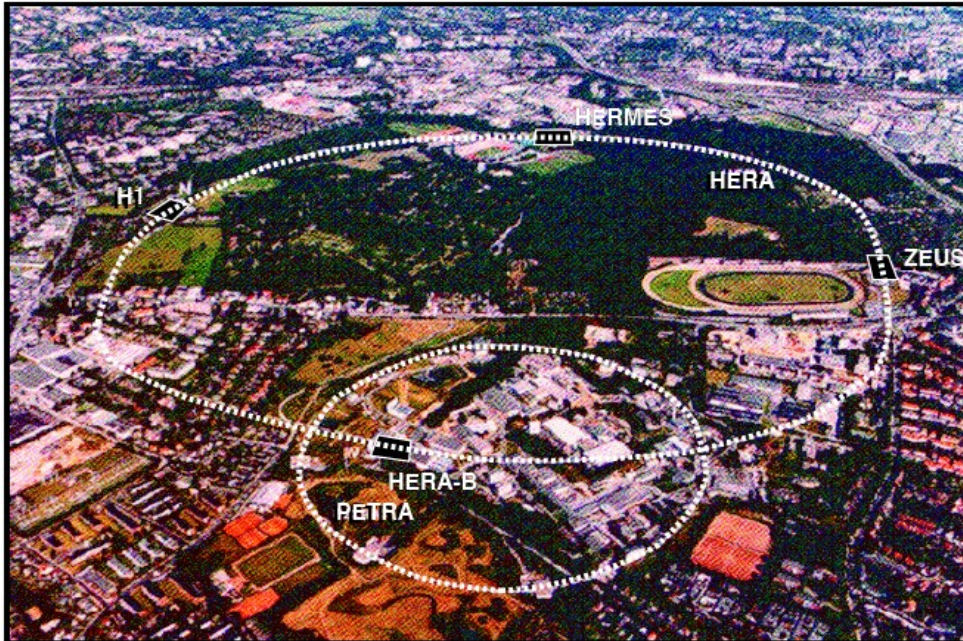
Inelasticity :

$$y = (q \cdot p)/(k \cdot p)$$



HERA overlaps with fixed-target, Tevatron and LHC experiments

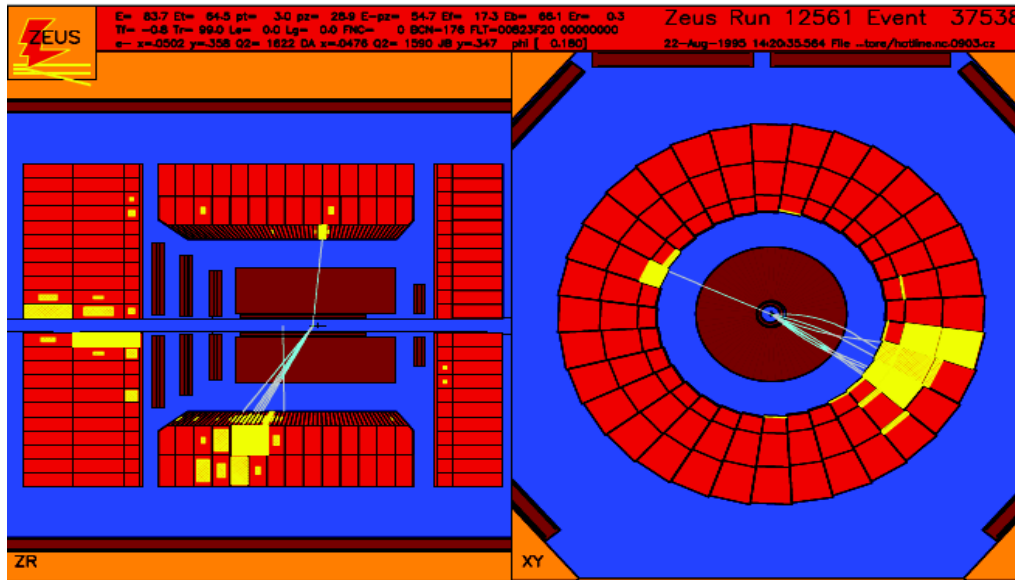
The HERA collider



- During 1992–2007, mainly $E_e = 27.5 \text{ GeV}$, $E_p = 920 \text{ GeV}$ giving $\sqrt{s} \sim 320 \text{ GeV}$; and dedicated data at different proton energies.
- Colliding-beam experiments collected combined sample $\sim 1 \text{ fb}^{-1}$.
- About 75% data taken with polarised ($\sim 30\%$) lepton beams, with equal amounts of e^- and e^+ and positive and negative polarisation.

6

DIS events in H1 and ZEUS

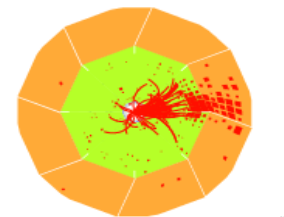


Charge current :

- Missing p_T from escaped neutrino
- Hadronic jet
- Reconstruction not as precise, larger backgrounds

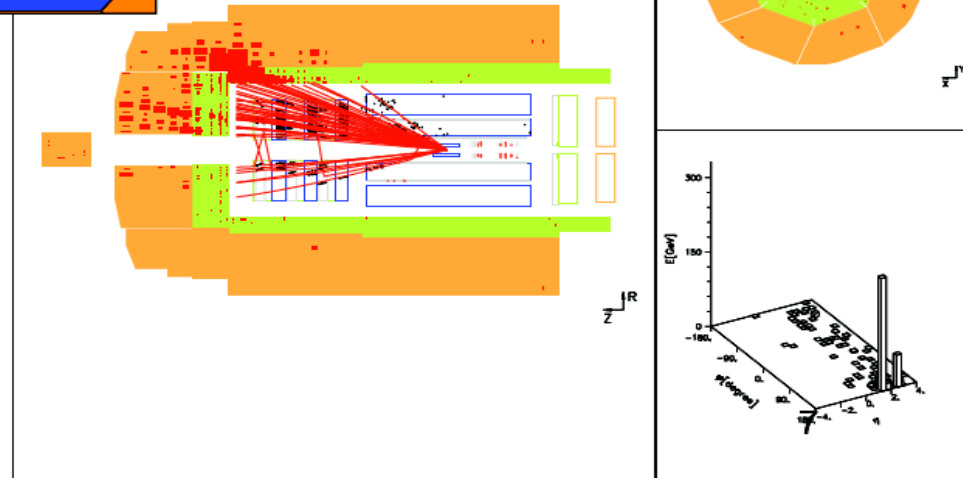
238837 Event 8595 Class: 4 5 6 7 11 19 25 26 28 run date 290399

9 Q2=41067 x=0.77 y=0.53

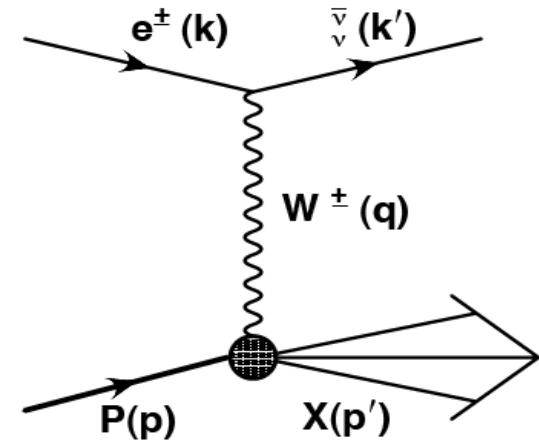
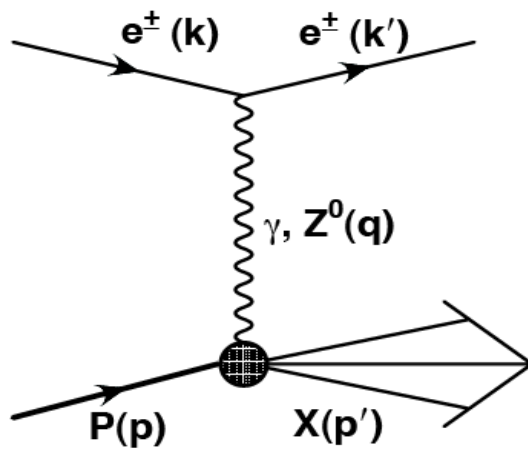


Neutral current :

- High energy isolated electron
- Back-to-back with hadronic jet
- Kinematics can be reconstructed in several ways, clean samples



Neutral and charged DIS processes



$$\frac{d^2\sigma^{e^\pm P}}{dx dQ^2} = \frac{2\pi\alpha^2}{xQ^4} \left[Y_+ F_2 \mp Y_- xF_3 - y^2 F_L \right]$$

$$\frac{d^2\sigma^{e^\pm P}}{dx dQ^2} = \frac{G_F^2}{2\pi} \frac{M_W^2}{Q^2 + M_W^2} \tilde{\sigma}^{e^\pm P}$$

$F_2 \sim$ **sum of q and \bar{q} densities**

$xF_3 \sim$ **density of valence quarks; from Z exchange**

$F_L \sim$ **gluon density**

$$\tilde{\sigma}^{e^+P} \sim (\bar{u} + \bar{c} + (1-y)^2(d + s))$$

$$\tilde{\sigma}^{e^-P} \sim (u + c + (1-y)^2(\bar{d} + \bar{s}))$$

Sensitive to individual quark flavours

Structure functions

$$\frac{d\sigma_{NC}^{\pm}}{dx dQ^2} = \frac{2\pi\alpha^2}{x} \left[\frac{1}{Q^2} \right]^2 \left[Y_+ \tilde{F}_2 \mp Y_- x \tilde{F}_3 - y^2 \tilde{F}_L \right]$$

$$\frac{d\sigma_{CC}^{\pm}}{dx dQ^2} = \frac{G_F^2}{4\pi x} \left[\frac{M_W^2}{M_W^2 + Q^2} \right]^2 \left[Y_+ \tilde{W}_2^{\pm} \mp Y_- x \tilde{W}_3^{\pm} - y^2 \tilde{W}_L^{\pm} \right]$$

$$Y_{\pm} = 1 \pm (1-y)^2$$

$$\tilde{F}_2 \propto \sum (xq_i + x\bar{q}_i)$$

Dominant contribution

$$x\tilde{F}_3 \propto \sum (xq_i - x\bar{q}_i)$$

Only sensitive at high $Q^2 \sim M_Z^2$

$$\tilde{F}_L \propto \alpha_s \cdot xg(x, Q^2)$$

Only sensitive at low Q^2 and high y

similarly for pure weak CC analogues:

$$W_2^{\pm}, xW_3^{\pm} \text{ and } W_L^{\pm}$$

The NC reduced cross section defined as:

$$\tilde{\sigma}_{NC}^{\pm} = \frac{Q^2 x}{2\alpha\pi^2} \frac{1}{Y_+} \frac{d^2\sigma^{\pm}}{dx dQ^2}$$

$$\tilde{\sigma}_{NC}^{\pm} \sim \tilde{F}_2 \mp \frac{Y_-}{Y_+} x\tilde{F}_3$$

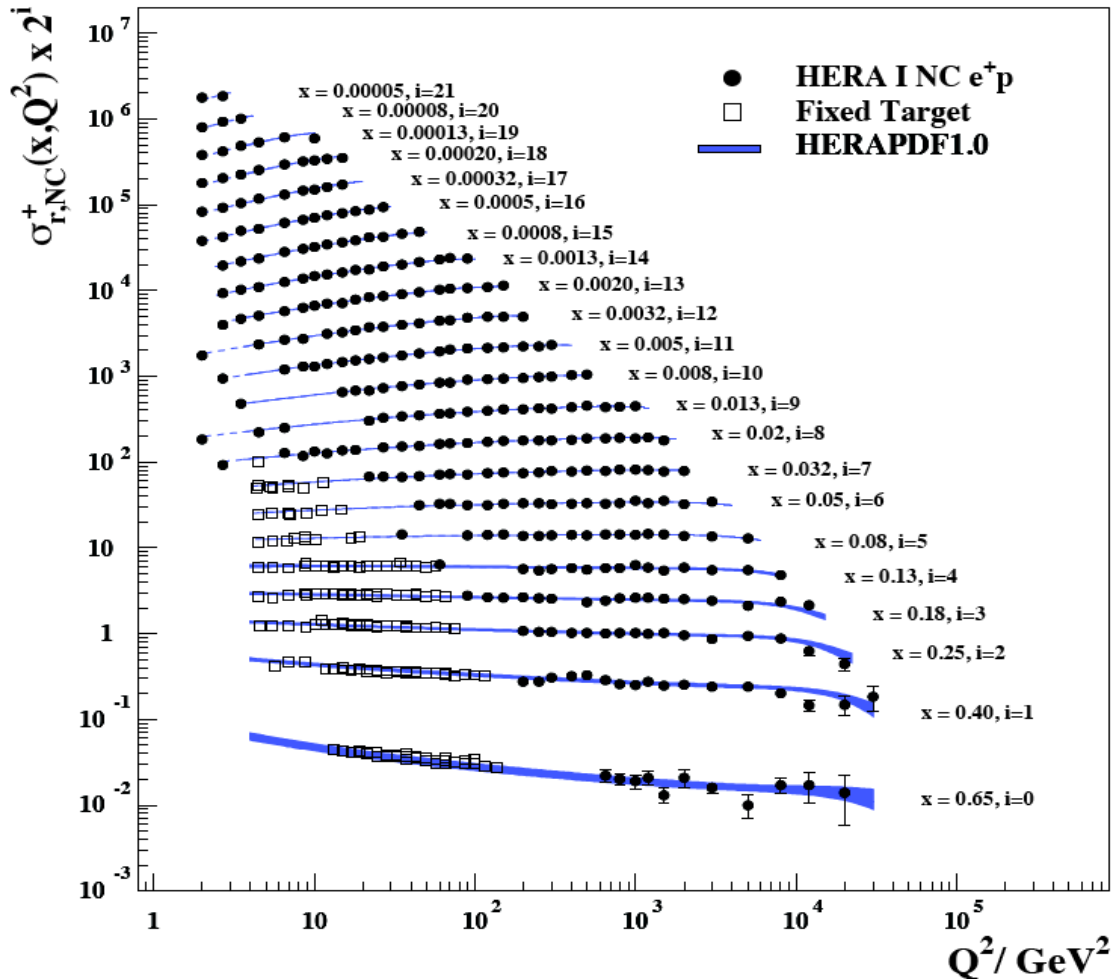
The CC reduced cross section defined as:

$$\sigma_{CC}^{\pm} = \frac{2\pi x}{G_F^2} \left[\frac{M_W^2 + Q^2}{M_W^2} \right]^2 \frac{d\sigma_{CC}^{\pm}}{dx dQ^2}$$

$$\frac{d\sigma_{CC}^{\pm}}{dx dQ^2} = \frac{1}{2} \left[Y_+ W_2^{\pm} \mp Y_- xW_3^{\pm} - y^2 W_L^{\pm} \right]$$

Inclusive DIS data and HERAPDF fit

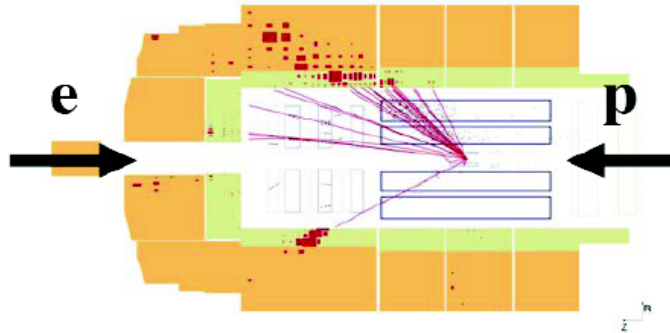
H1 and ZEUS



Impressive results for inclusive HERA I DIS data.

8

H1 and ZEUS



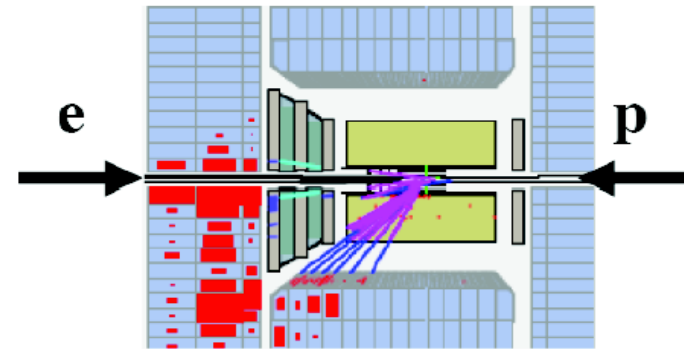
Neutral current event selection:

High P_T isolated scattered lepton
Suppress huge photo-production background by imposing longitudinal energy-momentum conservation

Kinematics may be reconstructed in many ways:
energy/angle of hadrons & scattered lepton provides excellent tools for sys cross checks

Removal of scattered lepton provides a high stats “pseudo-charged current sample”
Excellent tool to cross check CC analysis

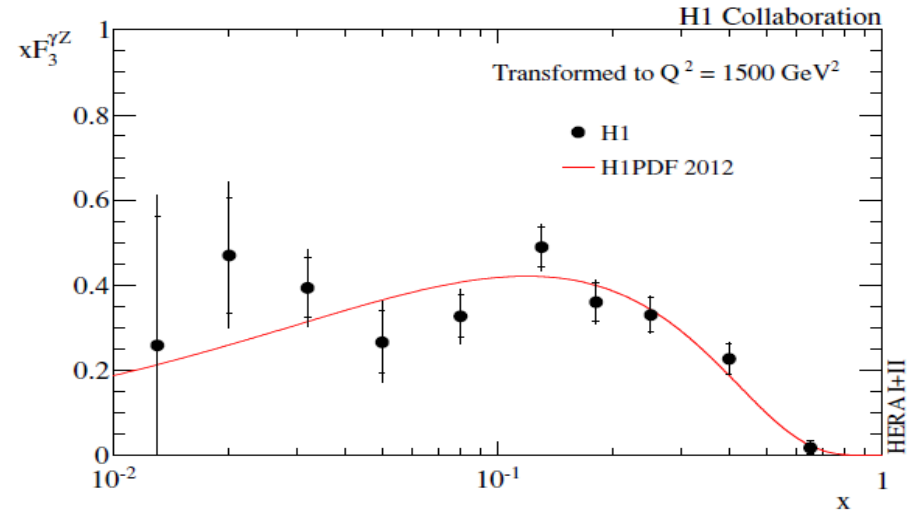
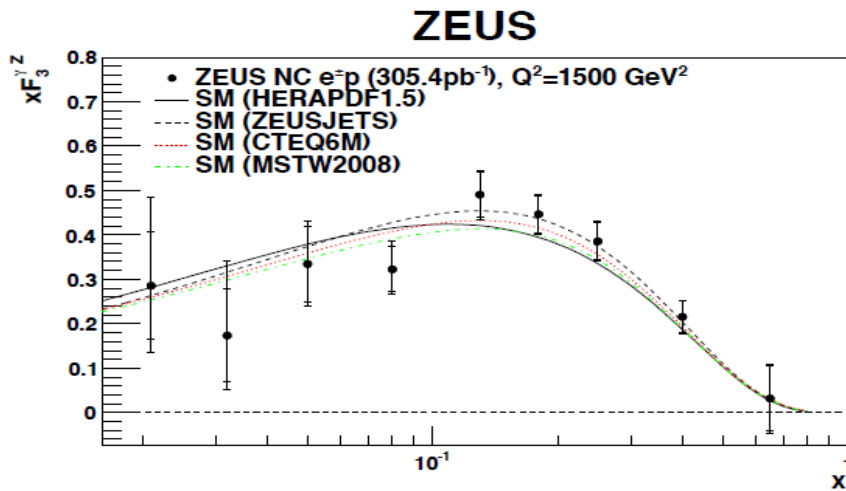
Final selection: $\sim 10^5$ events per sample at high Q^2
 $\sim 10^7$ events for $10 < Q^2 < 100 \text{ GeV}^2$



Charged current event selection:

Large missing transverse momentum (neutrino)
Suppress huge photo-production background
Topological finders to remove cosmic muons

Kinematics reconstructed from hadrons
Final selection: $\sim 10^3$ events per sample



At high Q^2 $x\tilde{F}_3$ arises due to Z^0 effects
 enhanced e^- cross section wrt e^+
 Difference is $x\tilde{F}_3$
 Sensitive to valence PDFs

$$x\tilde{F}_3 = \frac{Y_+}{2Y_-} (\tilde{\sigma}_{NC}^- - \tilde{\sigma}_{NC}^+) \approx a_e \chi_Z xF_3^{\gamma Z}$$

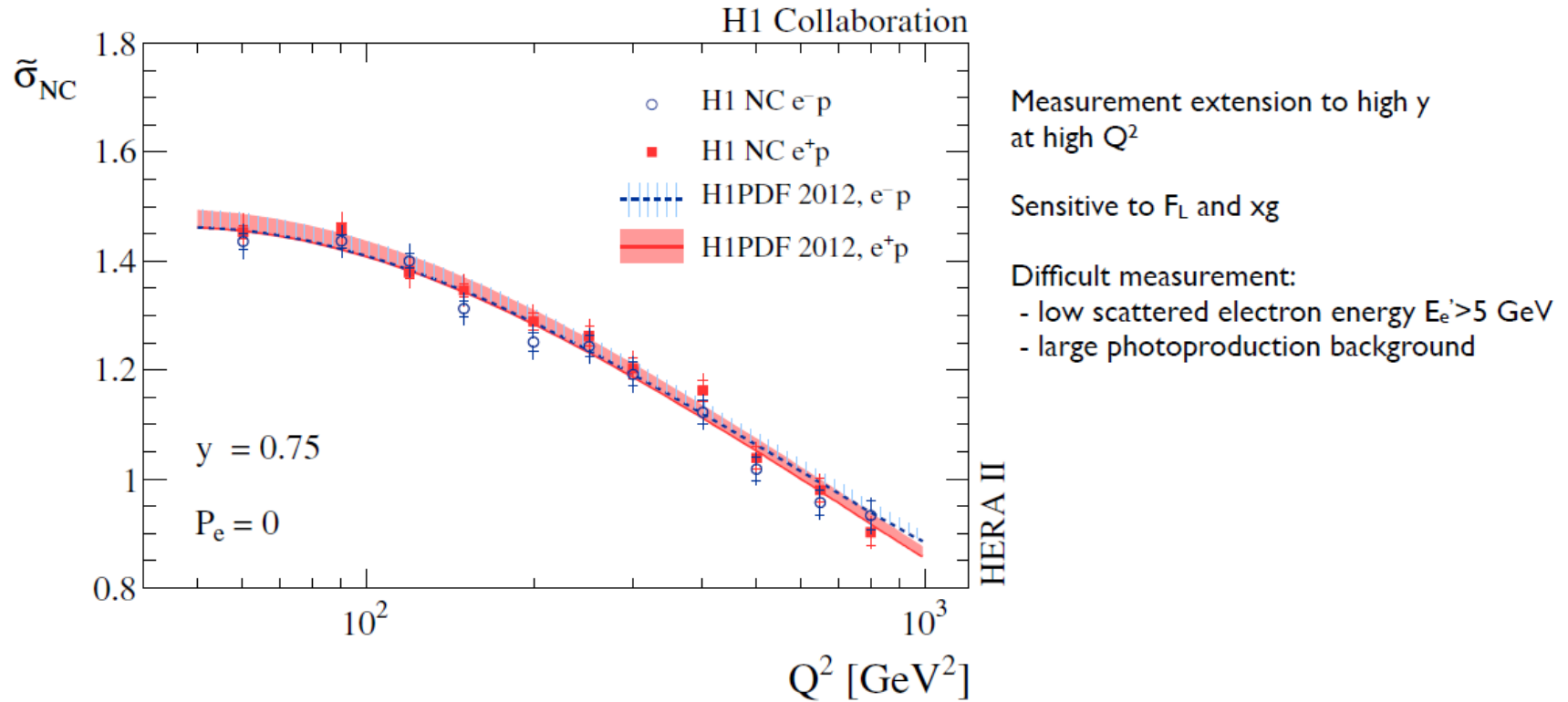
$$x\tilde{F}_3 \propto \sum (xq_i - x\bar{q}_i)$$

H1 measure integral of $x\tilde{F}_3^{\gamma Z}$ - validate sumrule:

$$\int_{0.016}^{0.725} dx F_3^{\gamma Z}(x, Q^2 = 1500 \text{ GeV}^2) = 1.22 \pm 0.09(\text{stat}) \pm 0.07(\text{syst})$$

NLO integral predicted to be $5/3 + \mathcal{O}(\alpha_s/\pi) = 1.16$

NC cross sections at high y



Measurement extension to high y
at high Q^2

Sensitive to F_L and xg

Difficult measurement:

- low scattered electron energy $E_e' > 5$ GeV
- large photoproduction background

Total uncertainty reduced by factor 2:

HERA-I ~4%

HERA-II ~2%

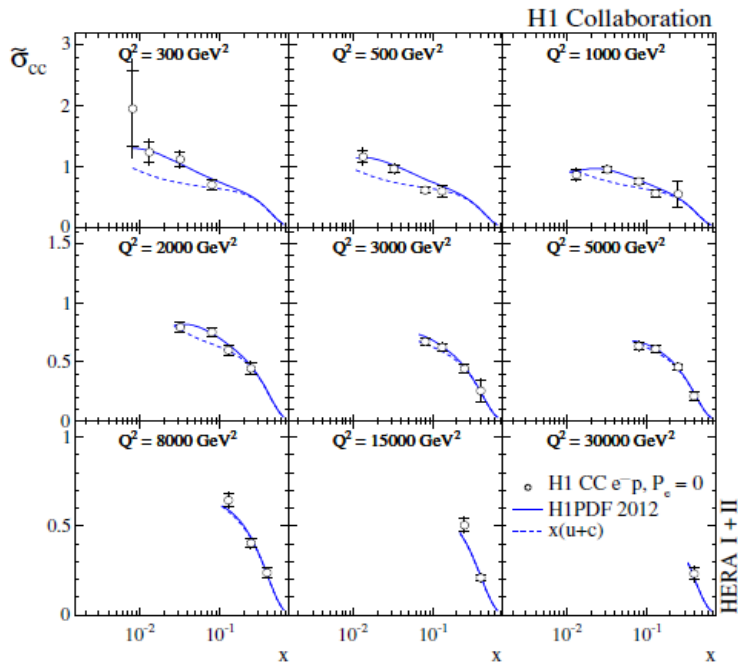
High Q^2 CC cross-section

Electron scattering

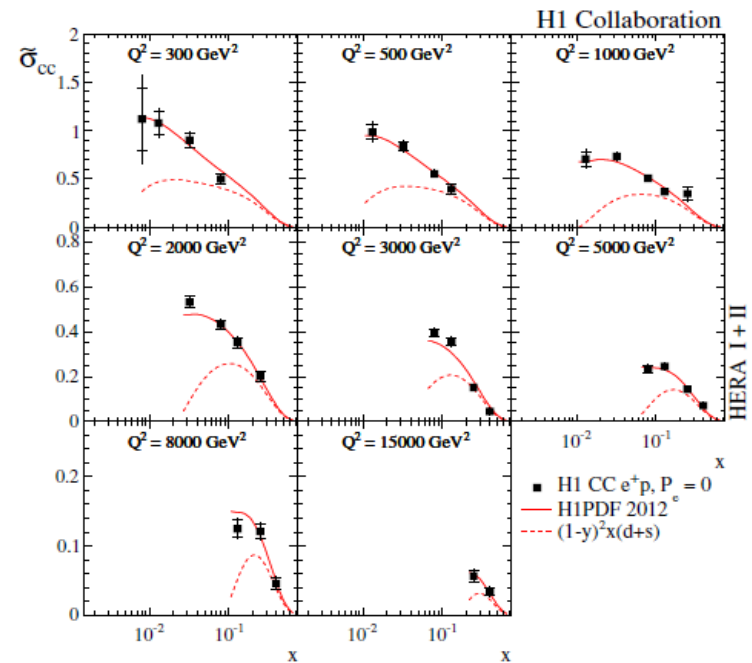
$$\frac{d^2\sigma_{CC}^-}{dx dQ^2} = \frac{G_F^2}{2\pi} \left(\frac{M_W^2}{M_W^2 + Q^2} \right)^2 \left[(u+c) + (1-y)^2(\bar{d} + \bar{s}) \right]$$

Positron scattering

$$\frac{d^2\sigma_{CC}^+}{dx dQ^2} = \frac{G_F^2}{2\pi} \left(\frac{M_W^2}{M_W^2 + Q^2} \right)^2 \left[(\bar{u} + \bar{c}) + (1-y)^2(d+s) \right]$$



H1 combination of high Q^2 CC data (HERA-I+II)
 Improvement of total uncertainty
 Dominated by statistical errors
 Provide important flavour decomposition information



CC e^+ data provide strong d_v constraint at high x
 Precision limited by statistics: typically 5-10%
 HERA-I precision of 10-15% for e^+
 Large gain to come after combination with ZEUS

H1PDF 2012

New PDF fit performed: can be thought of as a 'stepping-stone' towards HERAPDF2.0

$$xg(x) = A_g x^{B_g} (1-x)^{C_g} - A'_g x^{B'_g} (1-x)^{25},$$

$$xu_v(x) = A_{u_v} x^{B_{u_v}} (1-x)^{C_{u_v}} (1 + E_{u_v} x^2),$$

$$xd_v(x) = A_{d_v} x^{B_{d_v}} (1-x)^{C_{d_v}},$$

$$x\bar{U}(x) = A_{\bar{U}} x^{B_{\bar{U}}} (1-x)^{C_{\bar{U}}},$$

$$x\bar{D}(x) = A_{\bar{D}} x^{B_{\bar{D}}} (1-x)^{C_{\bar{D}}}.$$

Parameter	Central Value	Lower Limit	Upper Limit
f_s	0.31	0.23	0.38
m_c (GeV)	1.4	1.35 (for $Q_0^2 = 1.8$ GeV)	1.65
m_b (GeV)	4.75	4.3	5.0
Q_{\min}^2 (GeV ²)	3.5	2.5	5.0
Q_0^2 (GeV ²)	1.9	1.5 ($f_s = 0.29$)	2.5 ($m_c = 1.6, f_s = 0.34$)

13 parameter fit: additional flexibility given to u_v and d_v compared to H1PDF2009 / HERAPDF1.0

Apply momentum/counting sum rules:

$$\int_0^1 dx \cdot (xu_v + xd_v + x\bar{U} + x\bar{D} + xg) = 1$$

$$\int_0^1 dx \cdot u_v = 2 \quad \int_0^1 dx \cdot d_v = 1$$

Parameter constraints:

$$\begin{aligned} B_{\text{Ubar}} &= B_{\text{Dbar}} \\ \text{sea} &= 2 \times (\text{Ubar} + \text{Dbar}) \\ \text{Ubar} &= \text{Dbar at } x=0 \\ f_s &= \text{sbar/Dbar} \end{aligned}$$

$$Q_0^2 = 1.9 \text{ GeV}^2 \text{ (below } m_c)$$

$$Q^2 > 3.5 \text{ GeV}^2$$

$$2 \times 10^{-4} < x < 0.65$$

Fits performed using RT-VFNS

Experimental uncertainties produced using RMS spread of 400 replica fits

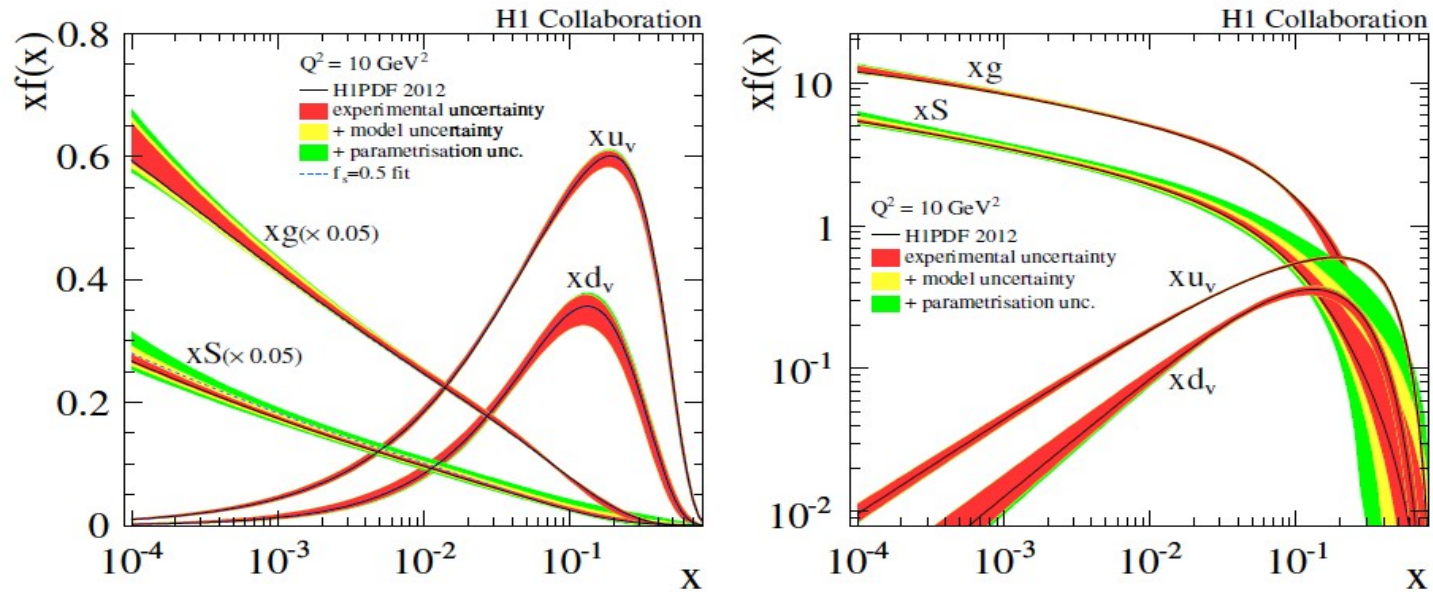
Parameterisation uncertainty determined from envelope of 14 parameter fit & Q_0^2 variations

Error band is applied to central value fit \Rightarrow asymmetric errors since mean of replicas \neq central fit

$$\chi^2 = \sum_i \frac{[\mu_i - m_i (1 - \sum_j \gamma_j^i b_j)]^2}{\delta_{i,\text{unc}}^2 m_i^2 + \delta_{i,\text{stat}}^2 \mu_i m_i (1 - \sum_j \gamma_j^i b_j)} + \sum_j b_j^2 + \sum_i \ln \frac{\delta_{i,\text{unc}}^2 m_i^2 + \delta_{i,\text{stat}}^2 \mu_i m_i}{\delta_{i,\text{unc}}^2 \mu_i^2 + \delta_{i,\text{stat}}^2 \mu_i^2}$$

modified χ^2 definition includes \ln term to account for likelihood transition to χ^2 after error scaling

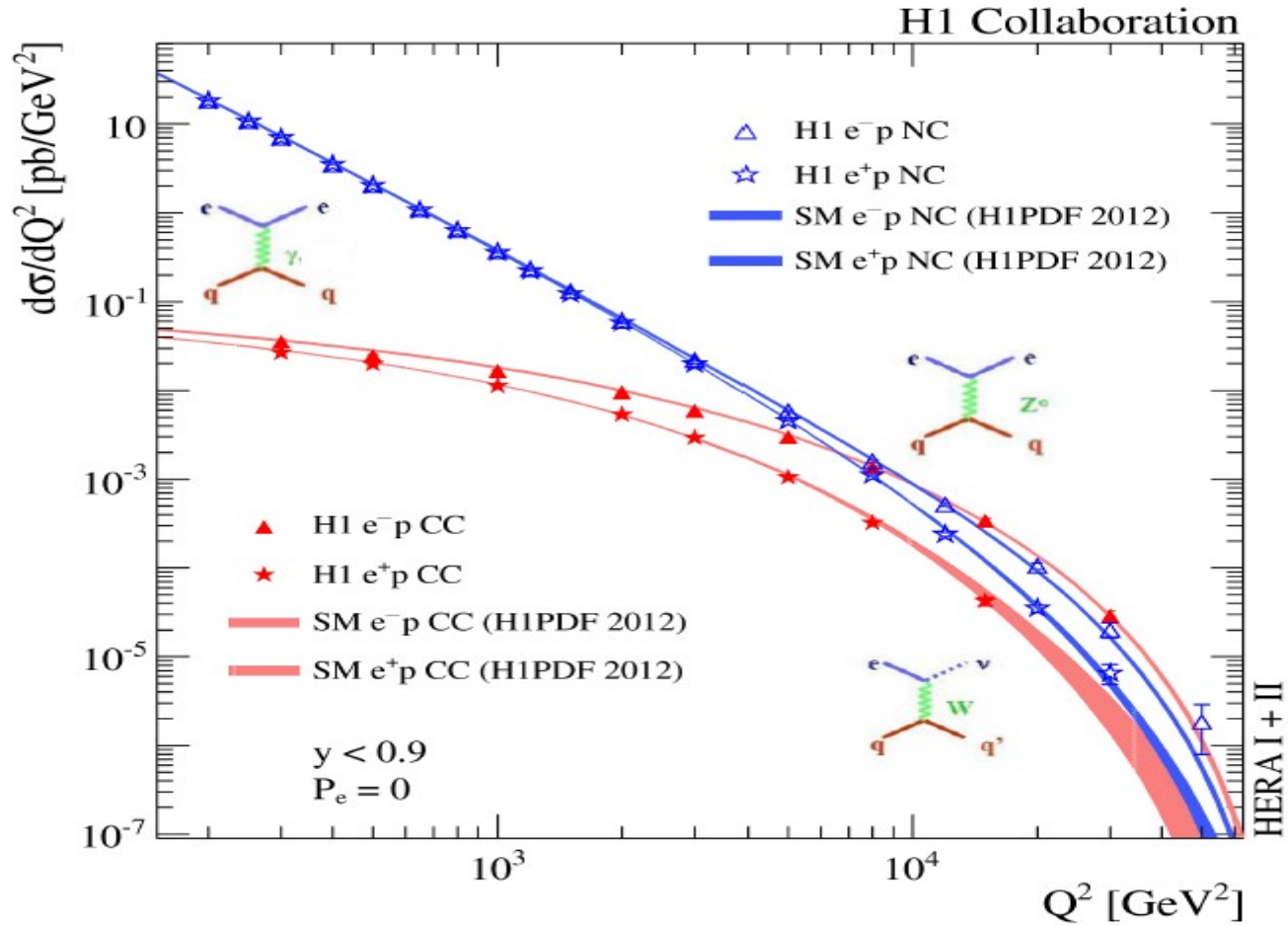
H1PDF 2012



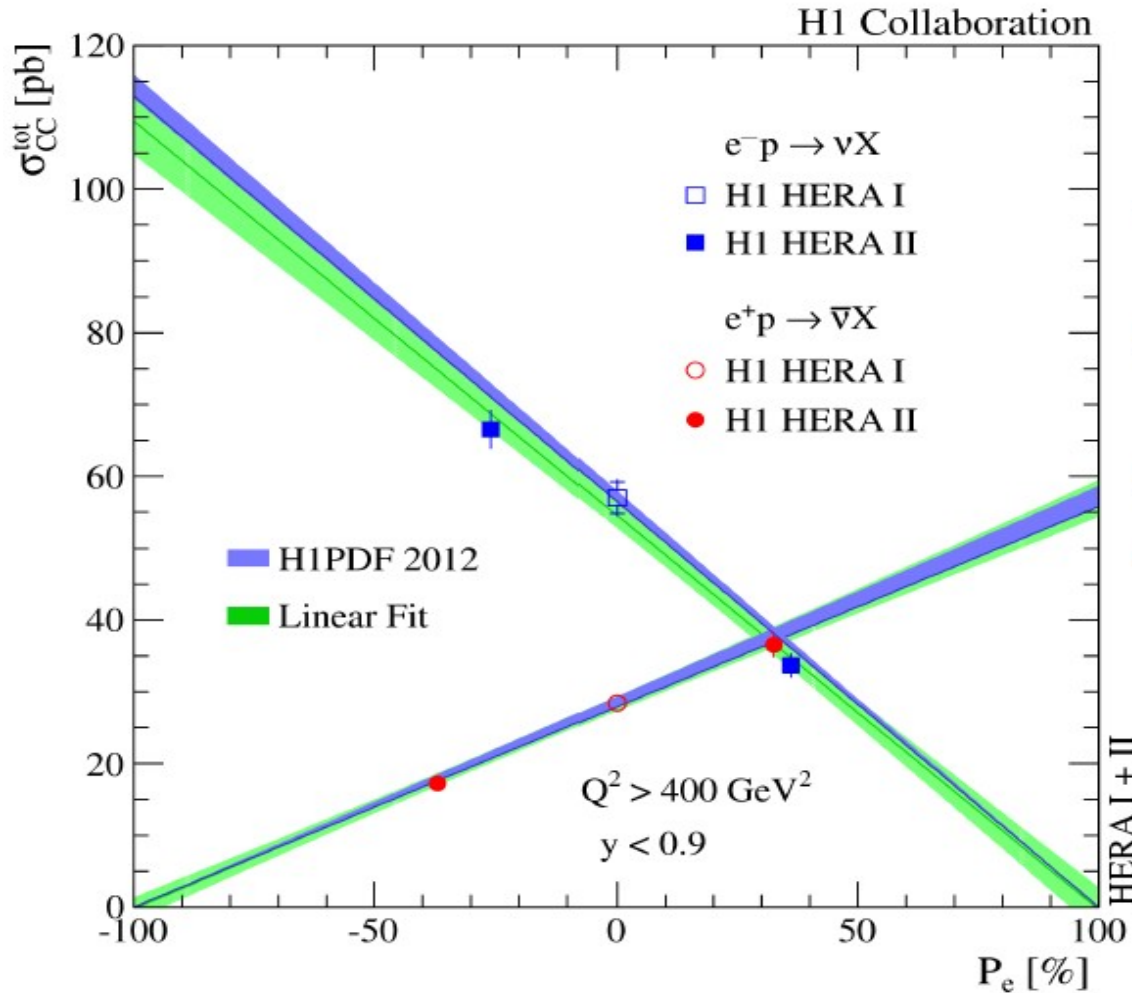
$$\chi^2/\text{ndf} = 1570/1461 = 1.07$$

Fit with unsuppressed strange sea ($f_s=0.5$) is well within error bands

Electroweak unification

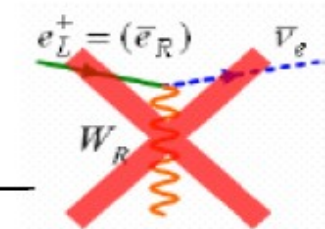


Parity violation in CC



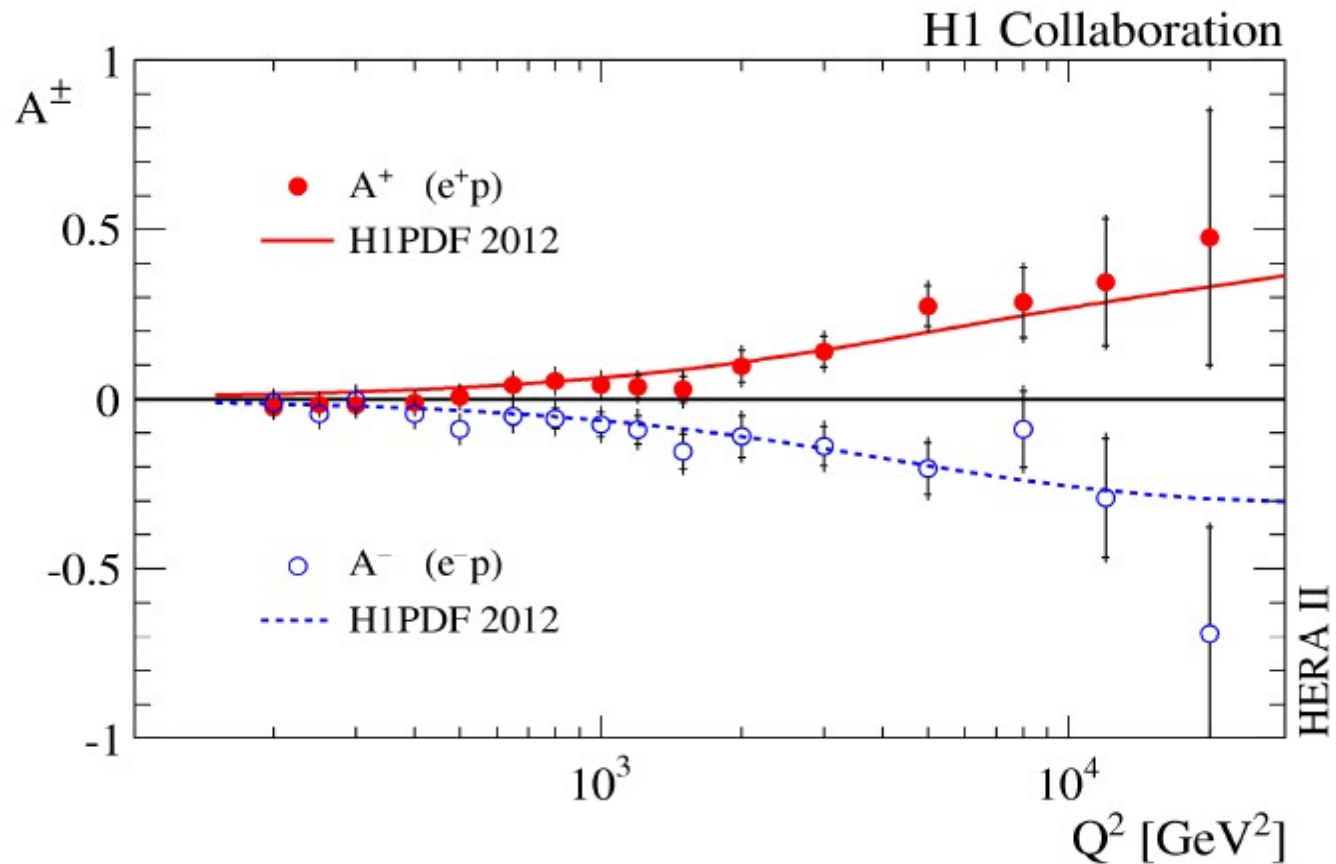
- Chiral structure of EW interactions probed
- SM CC:

$$\sigma_{cc}^{\pm}(P_e) = (1 \pm P_e)\sigma_{cc}^{\pm}(0)$$
- Agrees with theory
- Rules out $W_R < 200 \text{ GeV}$



Parity violation in NC

NC polarisation asymmetry $A^\pm = \frac{2}{P_L^\pm - P_R^\pm} \cdot \frac{\sigma^\pm(P_L^\pm) - \sigma^\pm(P_R^\pm)}{\sigma^\pm(P_L^\pm) + \sigma^\pm(P_R^\pm)}$



How PDF's are obtained?

- Choose a factorisation scheme (e.g. MSbar), and an order of perturbation theory (LO, NLO, NNLO) and a starting scale Q_0 where pQCD applies (e.g. 1-2 GeV).
- Parametrise quark and gluon distributions at Q_0 , e.g.

$$f_i(x, Q_0^2) = A_i x^{a_i} [1 + b_i \sqrt{x} + c_i x] (1 - x)^{d_i}$$

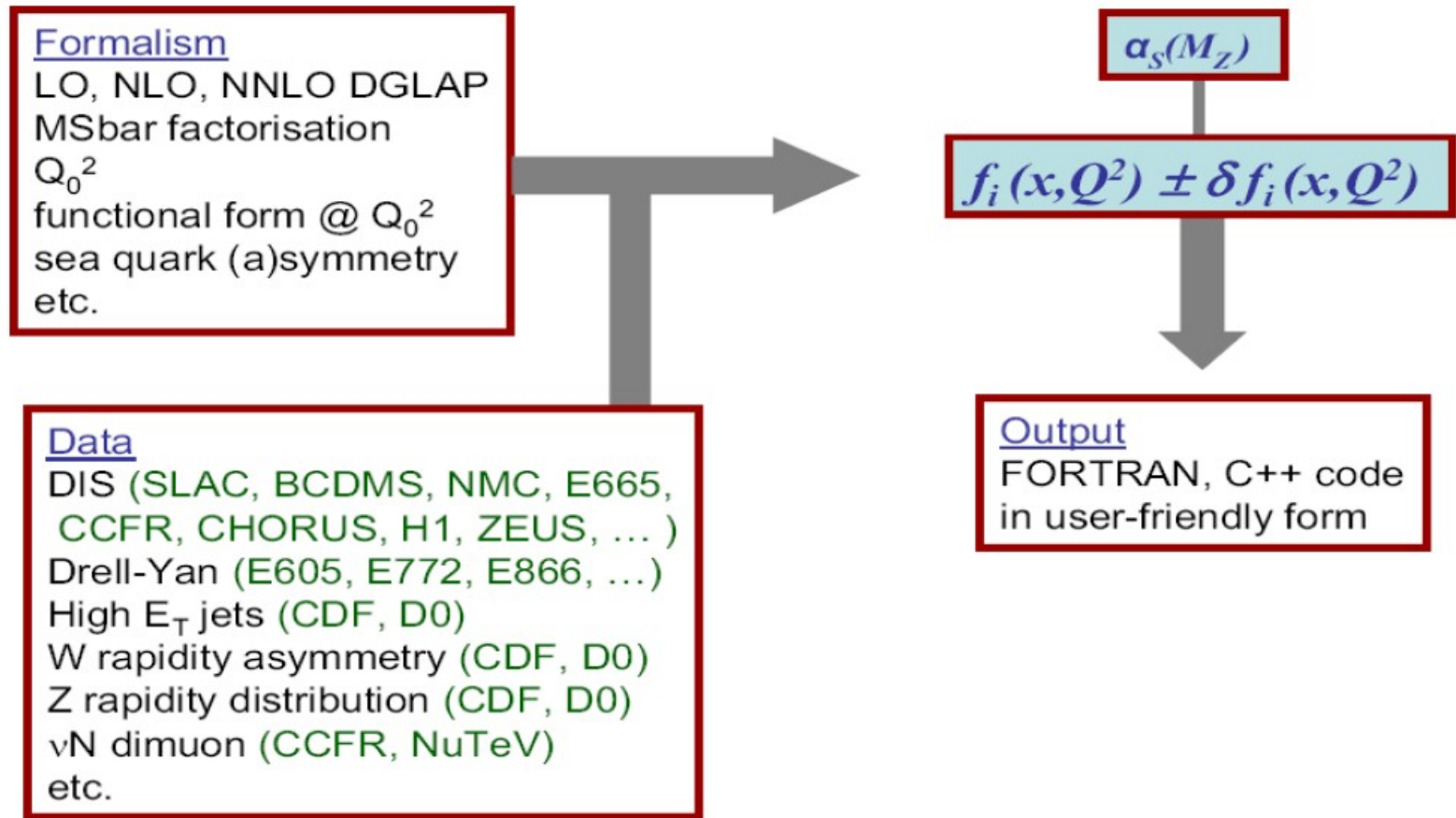
- Solve DGLAP equations to obtain the pdfs at any x and $Q > Q_0$; fit data for parameters ($A_i, a_i, \dots, \alpha_s$)
- Approximate the exact solutions (e.g. interpolation grids, expansions in polynomials etc), just output “global fit” is available for users

SUBROUTINE PDF (X, Q, U, UBAR, D, DBAR, ..., BBAR, GLU)

input

output

Anatomy of global PDF fit



Anatomy of global PDF fit

A starting scale of $Q_0^2 = 1.9 \text{ GeV}^2$ is used, parton distributions, as with the recent (fixed strange) fit to EW data are parameterised as

$$xu_v(x) = A_{u_v} x^{B_{u_v}} (1-x)^{C_{u_v}} (1 + E_{u_v} x^2)$$

$$xd_v(x) = A_{d_v} x^{B_{d_v}} (1-x)^{C_{d_v}}$$

$$x\bar{U}(x) = A_{\bar{U}} x^{B_{\bar{U}}} (1-x)^{C_{\bar{U}}}$$

$$x\bar{D}(x) = A_{\bar{D}} x^{B_{\bar{D}}} (1-x)^{C_{\bar{D}}}$$

$$xg(x) = A_g x^{B_g} (1-x)^{C_g} - A'_g x^{B'_g} (1-x)^{C'_g}$$

- where $\bar{D} = \bar{d} + \bar{s}$, A_{u_v} , A_{d_v} and A_g are fixed by sum rules, $C'_g = 25$ and the A and B parameters are the common for the u and d sea quarks to ensure $x\bar{u} = x\bar{d}$ as $x \rightarrow 0$

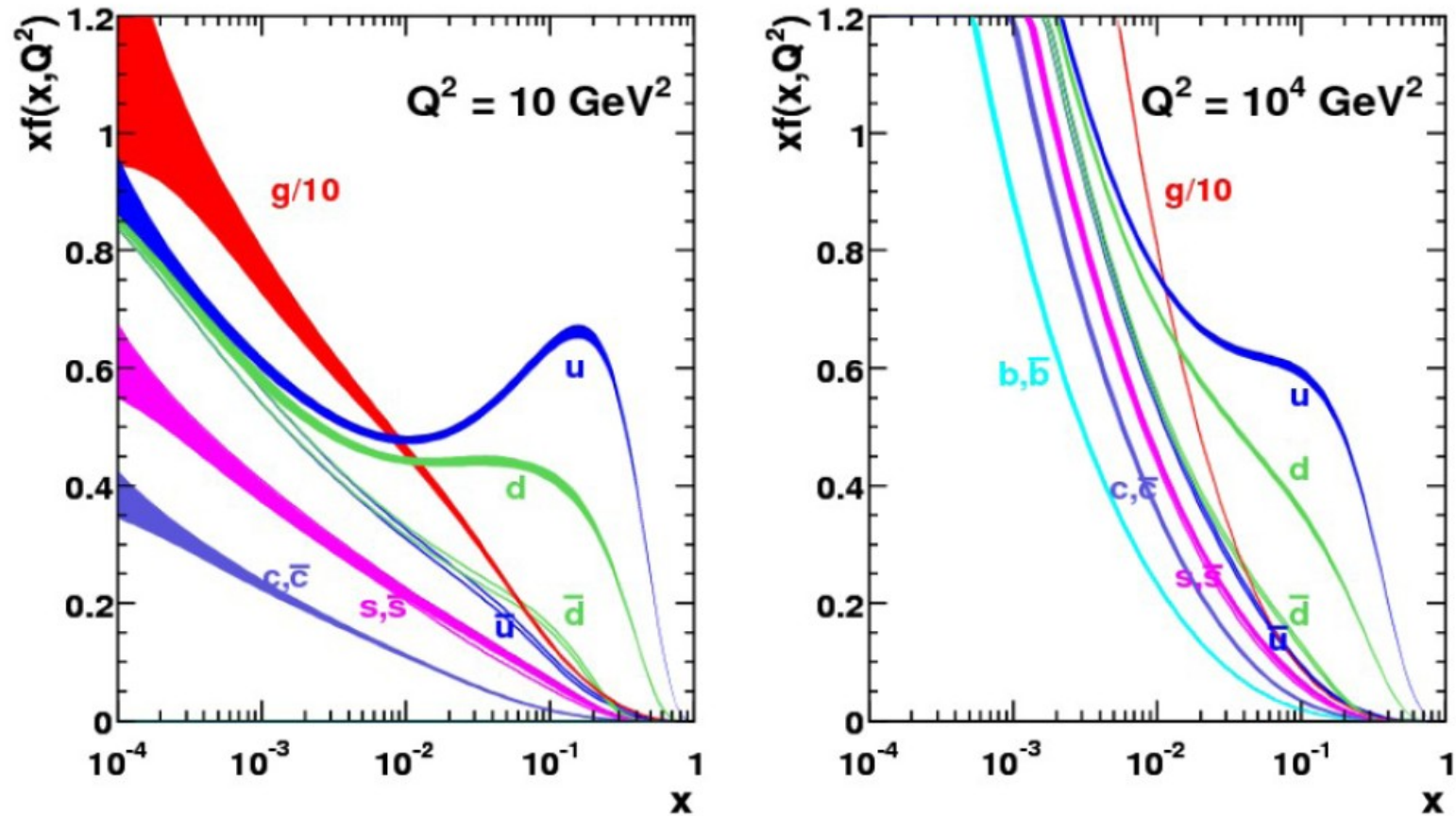
The strong coupling, $\alpha_s(M_Z) = 0.1176$

The Roberts-Thorne variable flavour number scheme is with charm mass is set to 1.4 GeV, and the bottom mass is 4.75 GeV

Uncertainties estimated using the Hessian method

Uncertainties from experimental uncertainties considered only - no model uncertainties

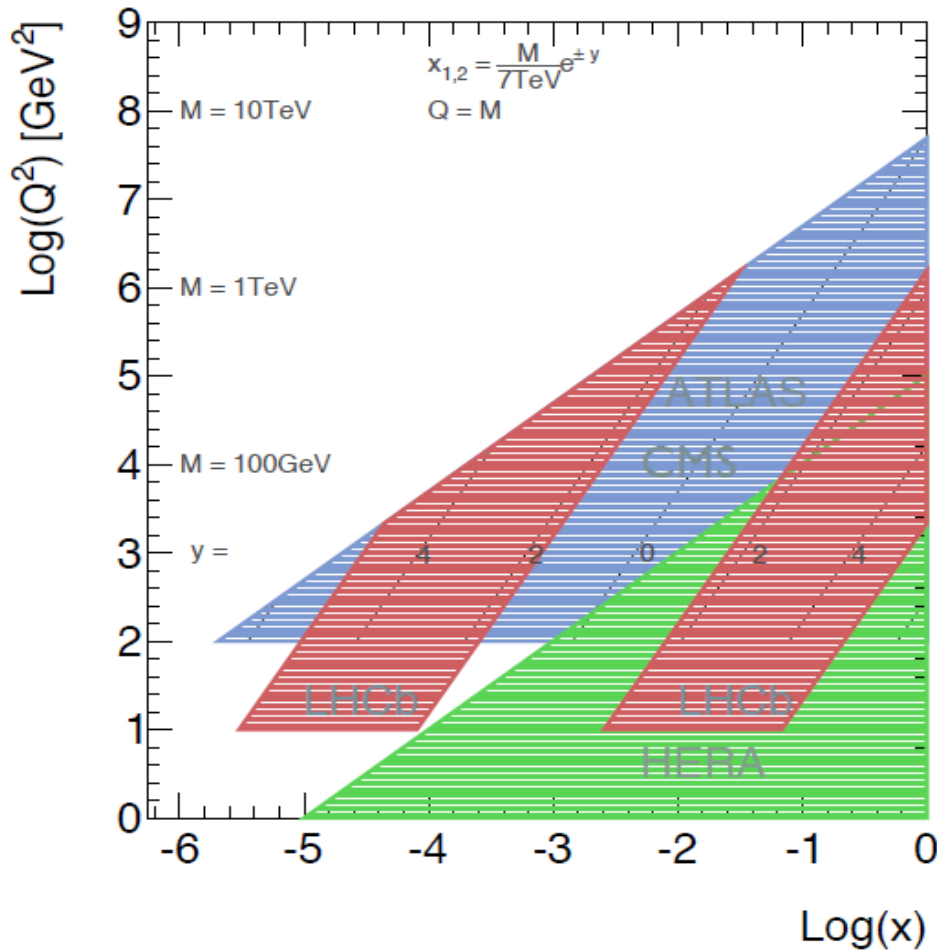
MSTW 2008 NLO PDFs (68% C.L.)



Symmary on HERA results

- H1 / ZEUS completed their final SF measurements
- New HERA-II data provide tighter constraints at high x / Q^2
- These data provide some of the most stringent constraints on PDFs
- Stress-test of QCD over 4 orders of mag. in Q^2
- DGLAP evolution works very well
- HERA data provide a self-consistent data set for complete flavour decomposition of the proton
- New combination of HERA data underway
- Combination \Rightarrow HERAPDF2.0 QCD fit

Kinematics at LHC



LHC: largest mass states at large x

For central production $x=x_1=x_2$

$$M = x\sqrt{s}$$

i.e. $M > 1\text{TeV}$ probes $x > 0.1$

Searches for high mass states require precision knowledge at high x

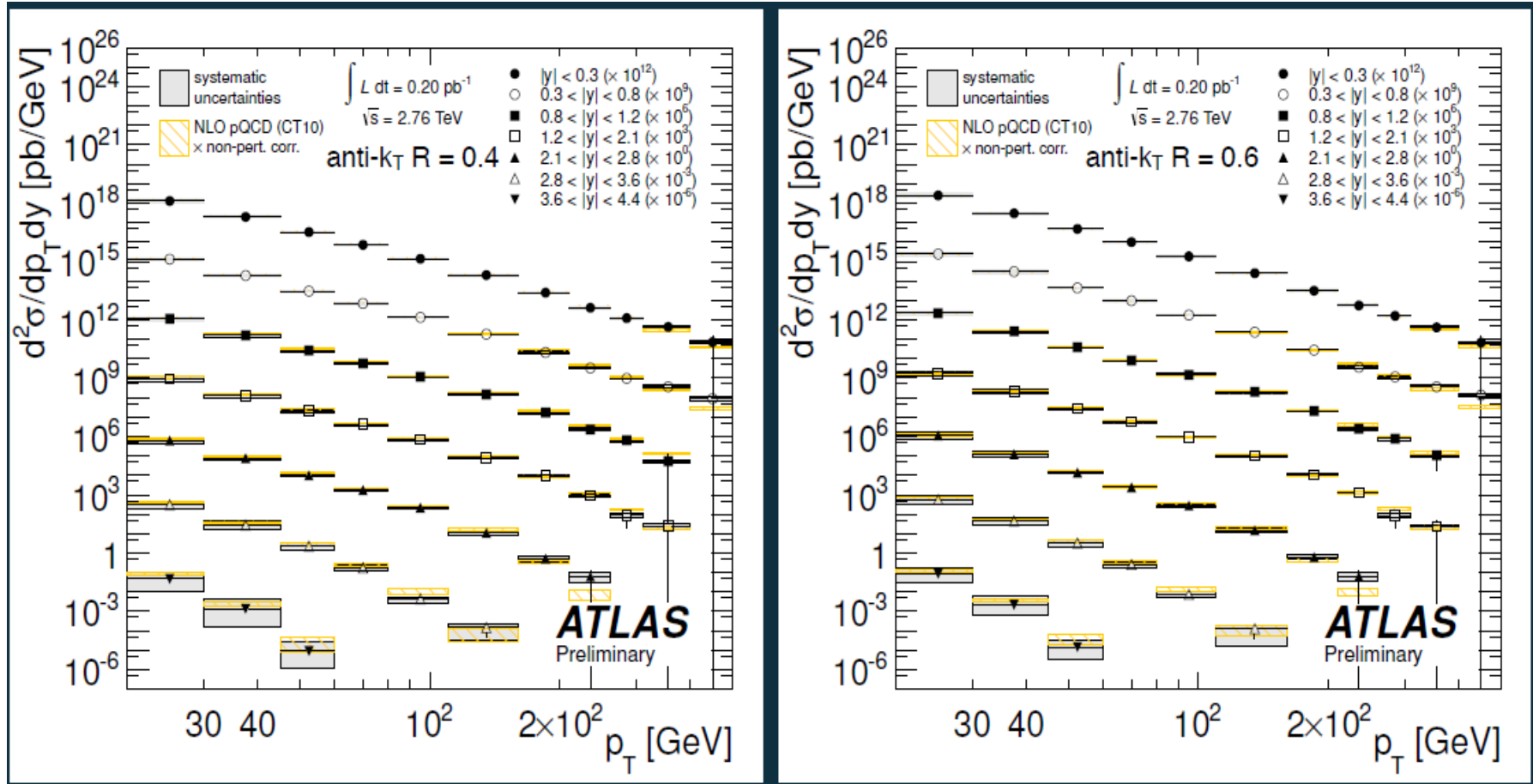
Z' / quantum gravity / susy searches...

DGLAP evolution allows predictions to be made

High x predictions rely on

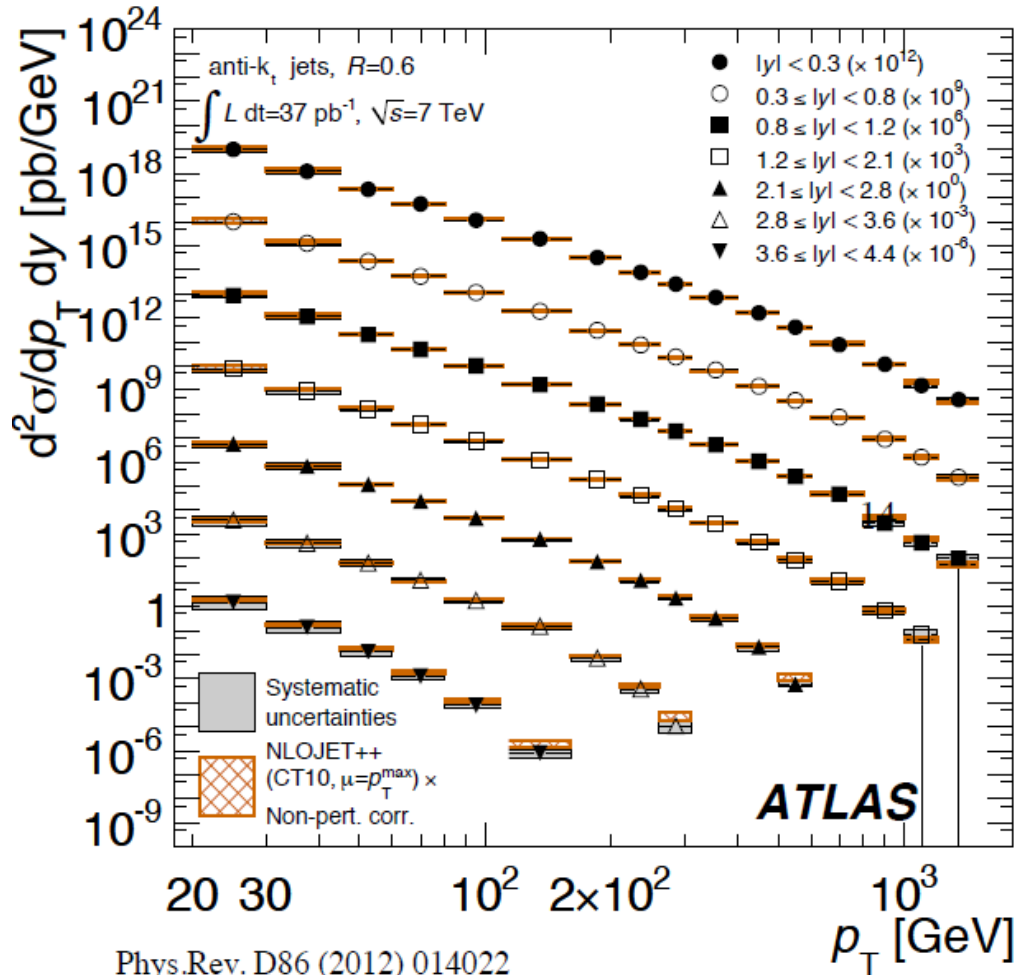
- data (DIS / fixed target)
- sum rules
- behaviour of PDFs as $x \rightarrow 1$

The jet cross-section at 2.76 TeV



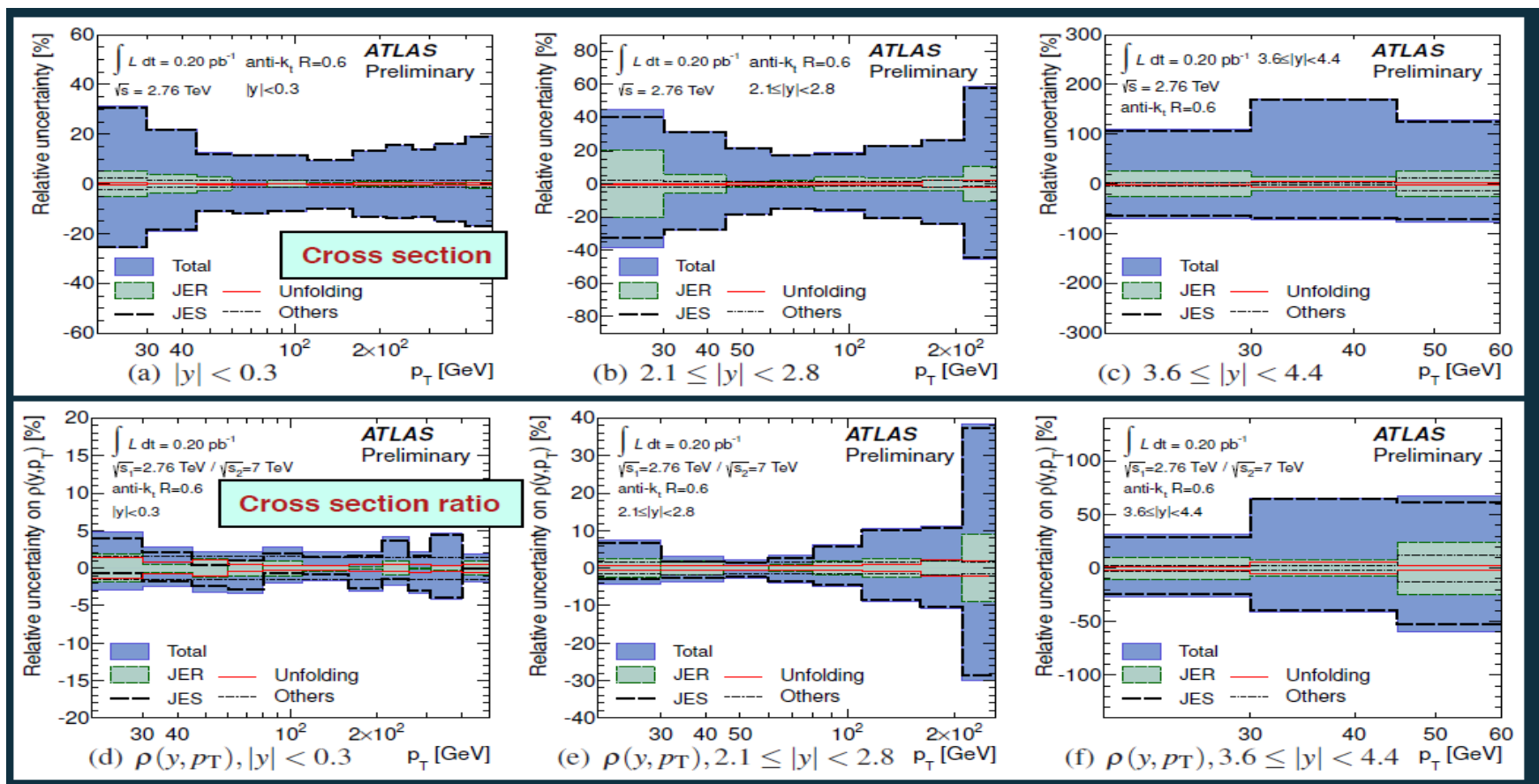
- Data from ATLAS-CONF-2012-128, two anti- k_T radii; 0.4 and 0.6
- Again a good agreement of the NLO prediction over 7 orders of magnitude within the experimental uncertainty (2.8% preliminary luminosity uncertainty not shown)

The jet cross-section at 7 TeV



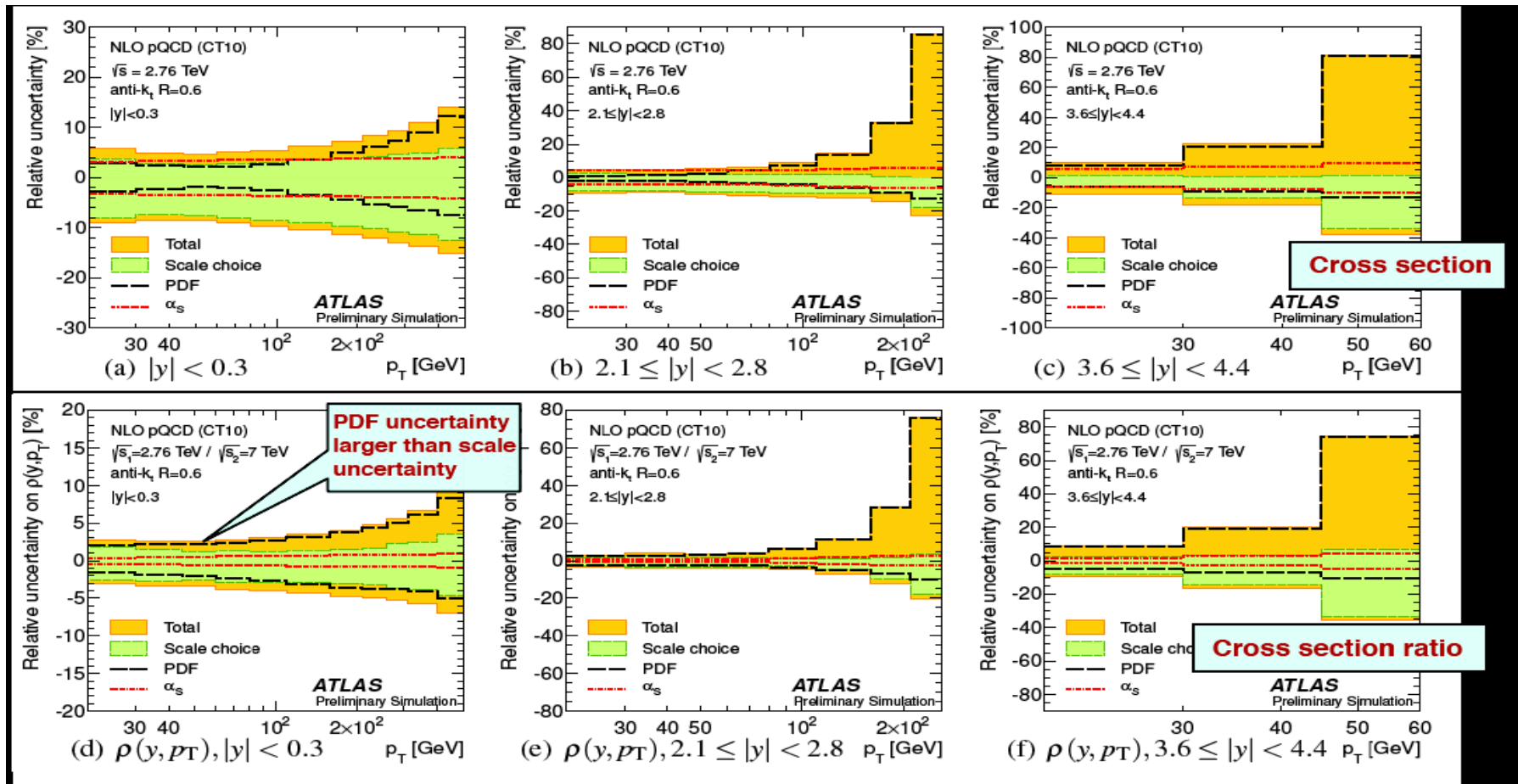
- Statistically precise determination of the inclusive jet cross section with jet p_T up to 1.5 TeV from 37 pb^{-1} of data
- Agreement with perturbative QCD over more than 8 orders of magnitude
- Large systematic uncertainties, may not be so constraining in a PDF fit at NLO (Luminosity uncertainty of 3.4% not shown)

Uncertainties on the ratio 2.76 to 7 TeV



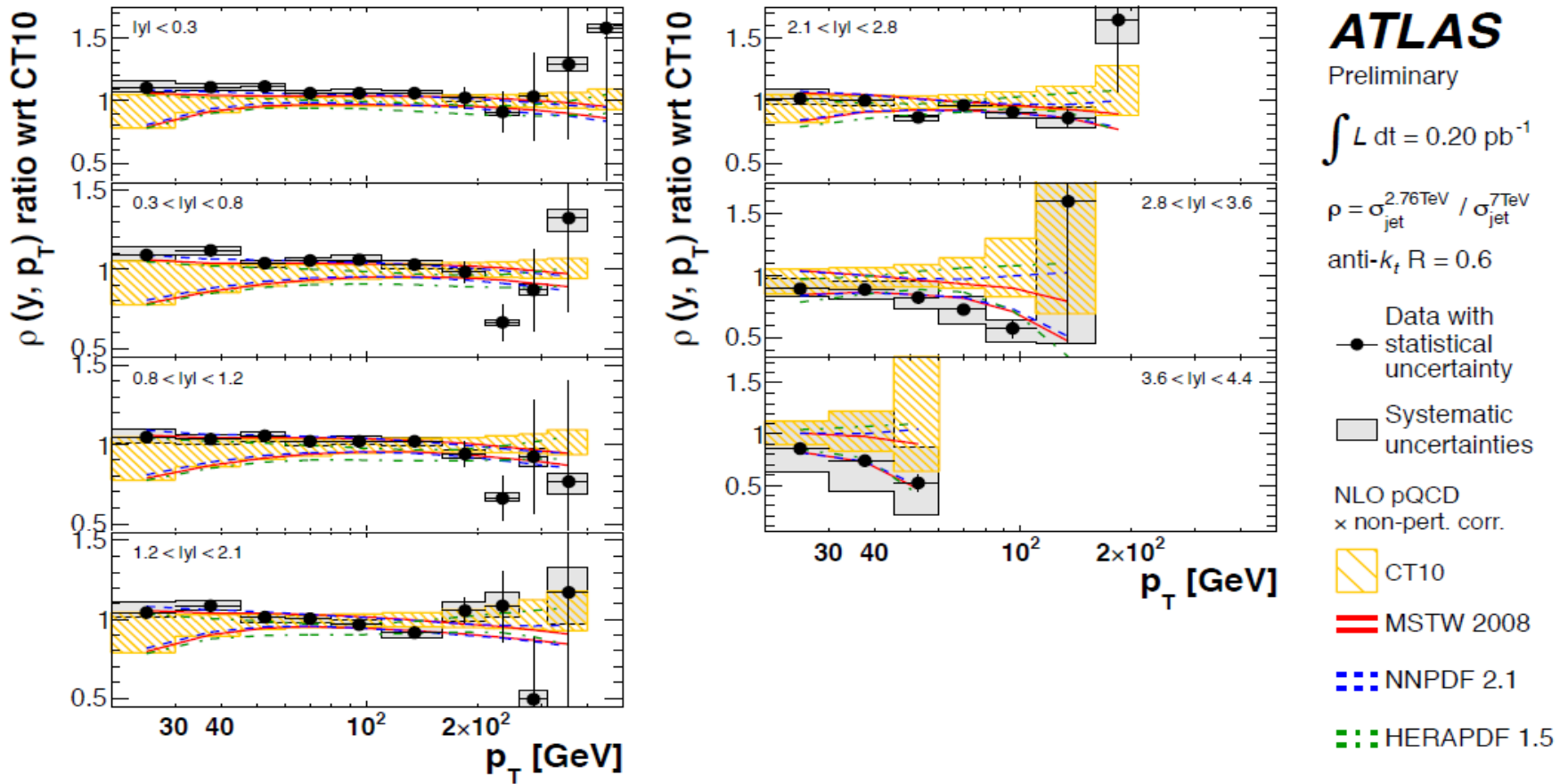
Experimental uncertainties on the ratio better than 5% in the central region - better than 30% in the forward region at low p_T

PDF uncertainties on the ratio 2.76 to 7 TeV



- Corresponding bins in p_T at 2.76 TeV and 7 TeV will correspond to different regions of x and Q^2
- Still gives rise to significant - albeit smaller - PDF uncertainties

Ratio vs theory



- With the ratio the experimental uncertainties are generally smaller than the PDF uncertainty - particularly at low p_T

HERA + ATLAS global PDF fits

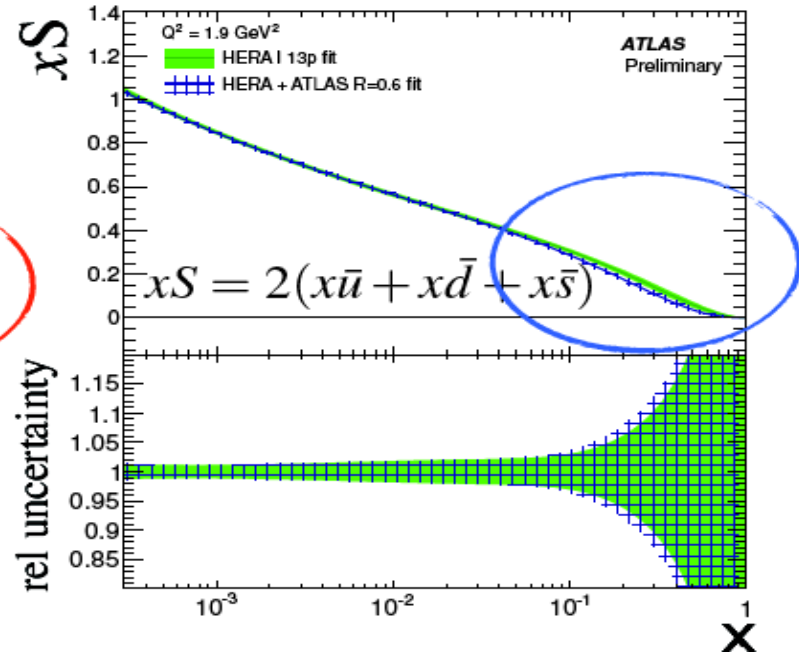
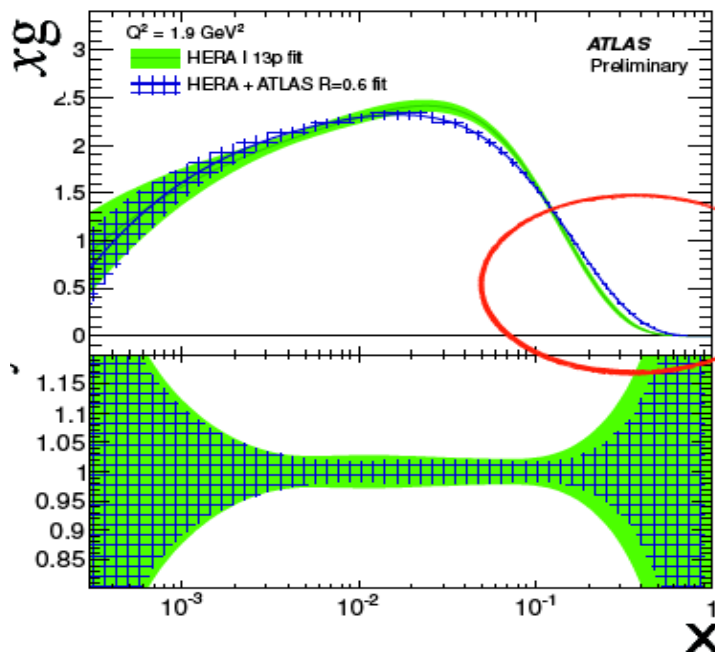
Different centre-of-mass energies probe different x and Q^2 values for the same p_T and rapidity ranges.

➔ Increased sensitivity to PDFs expected when both sets of jet cross section data are analyzed together

After inclusion of the ATLAS jet data:

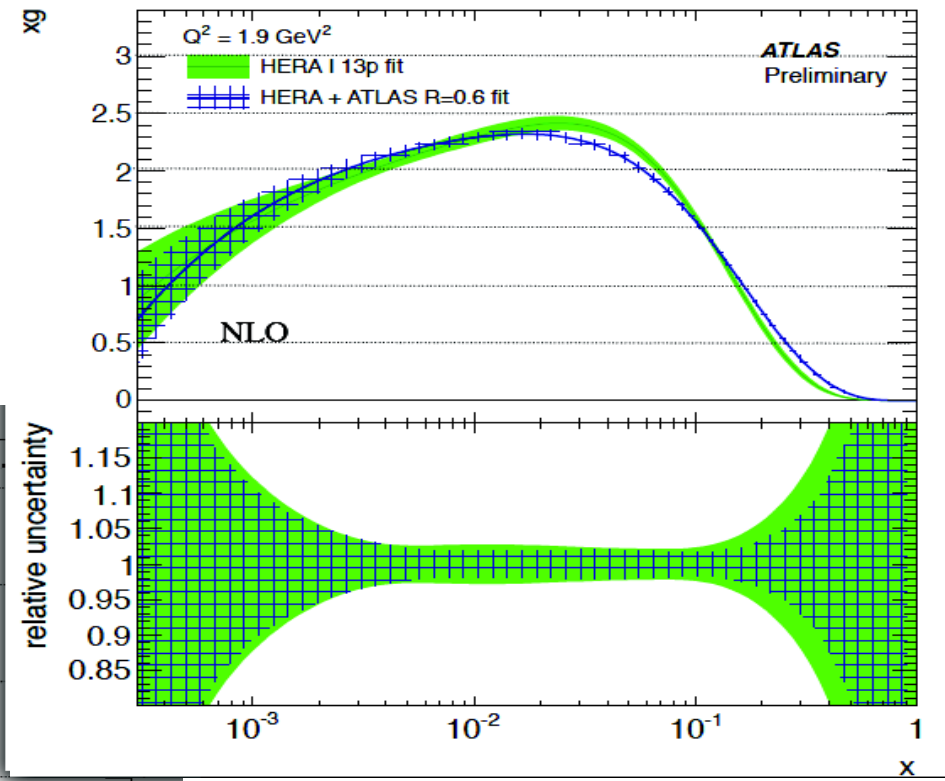
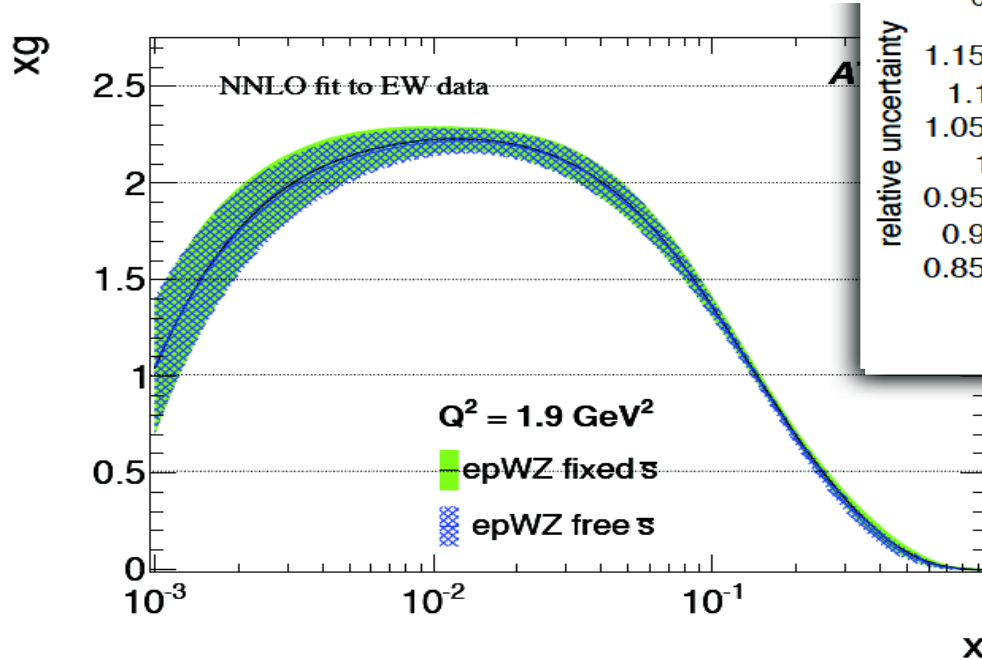
➔ gluon distribution (xg) tends to be **harder** with a reduction in the uncertainty

➔ sea quark distribution (xS) tends to be **softer** for high x resulting in a larger uncertainty



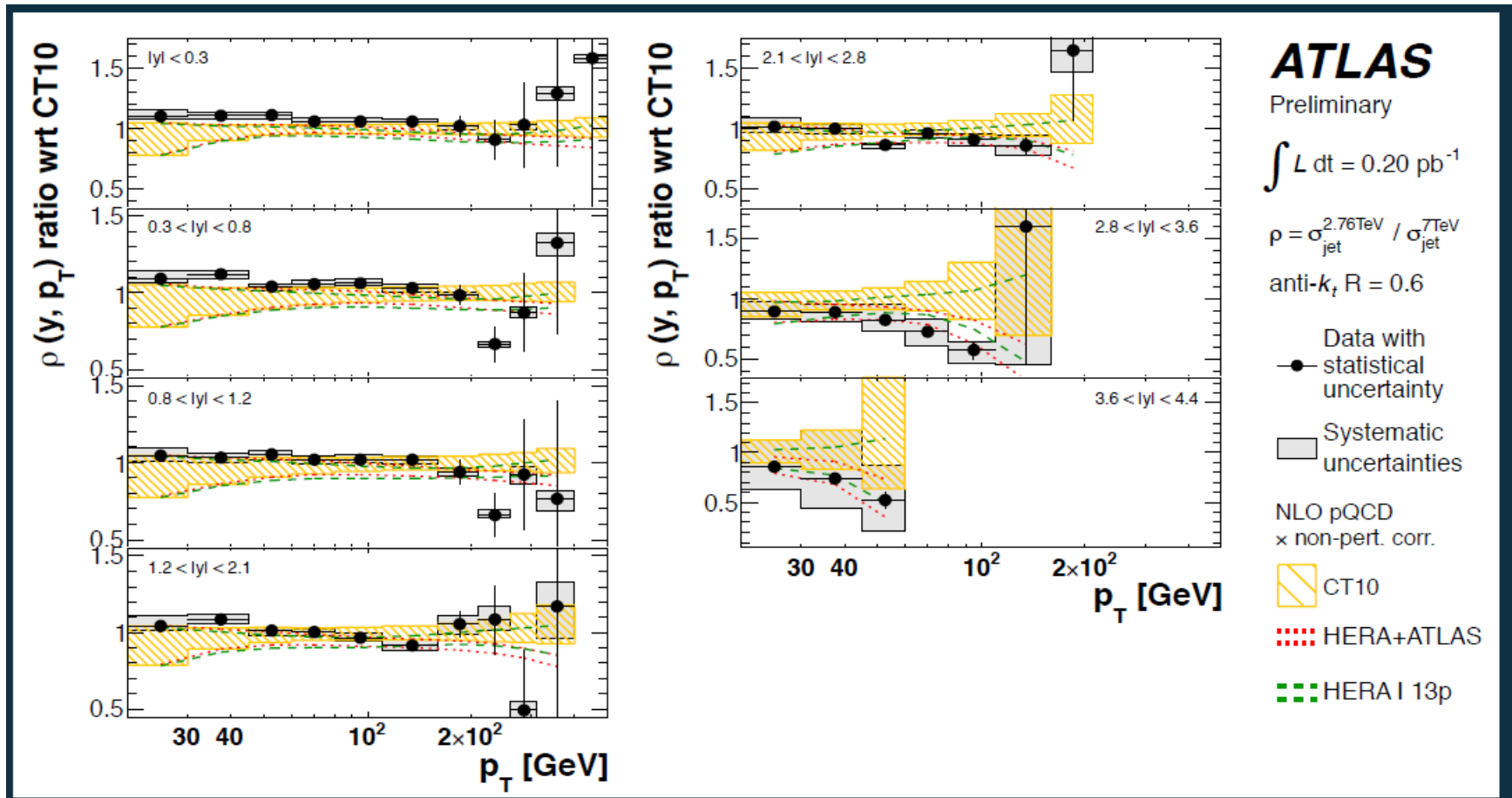
HERA + ATLAS global PDF fits

Here include also ATLAS electroweak data



- NNLO Fits to Electroweak boson production, although cannot be compared directly, do seem to support a harder gluon distribution

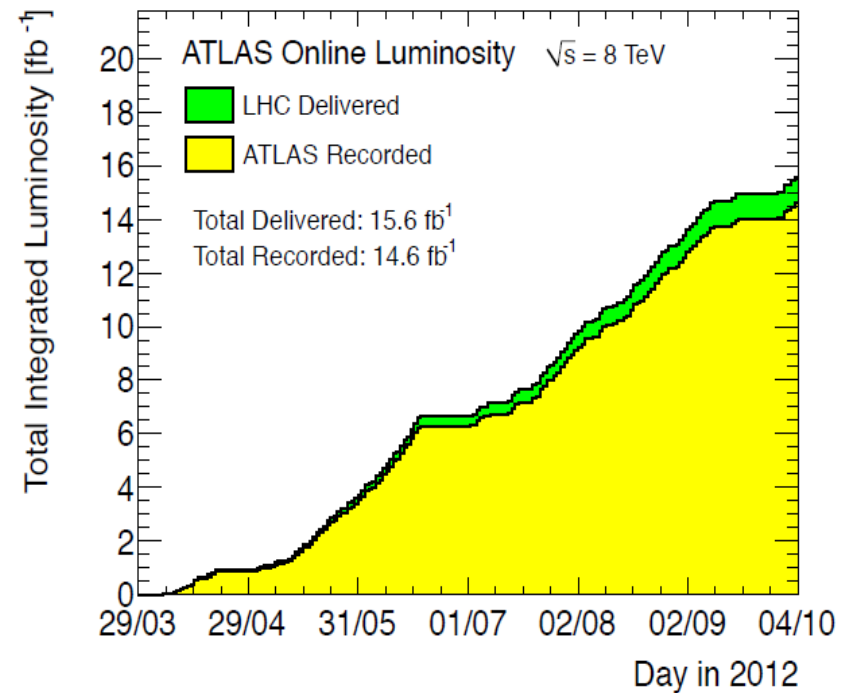
Comparison with the ratio



Again the fits agree well with the data, with the HERA+ATLAS fit agreeing better in the forward region

Outlook

- The cross section at lower p_T centre of mass energy, 2.76 TeV has been measured
- Except at the highest jet p_T , the data are systematics limited
- Fits to the data have been performed taking account of the correlated experimental uncertainties
- The fits predict a harder gluon distribution with a significantly (30%) reduction in the uncertainty



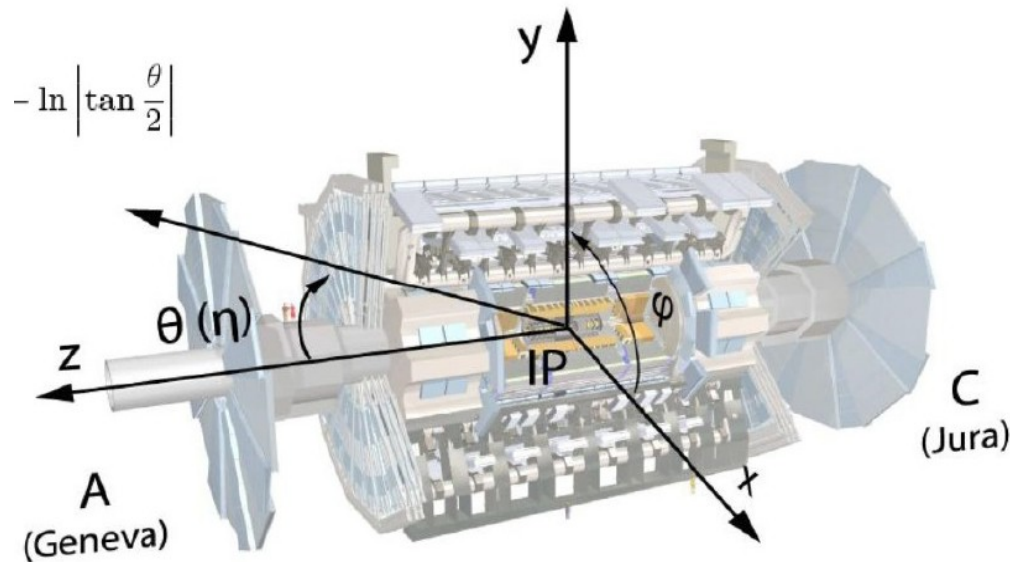
- The LHC has been performing exceptionally well, with over 14 fb⁻¹ of data collected at 8 TeV centre-of-mass energy
- This will allow better precision, even at the highest p_T where the data are currently statistics limited

Next topics

- 7.11 - W, Z bosons: inclus. cross-sections, W/Z+jets
- 14.11 - W, Z bosons: precise measurements
- 21.11 - Top: xsection, mass
- 28.11 - Dibosons and anomalous couplings
- 5.12, 12.12 - **Higgs**
- 19.12 - **SUSY**
- 9.1 - other searches for New Physics
- 16.1 - B-physics programme
- 23.1 - heavy ion programme

ATLAS Detector

THE ATLAS DETECTOR IS
REALLY BIG!

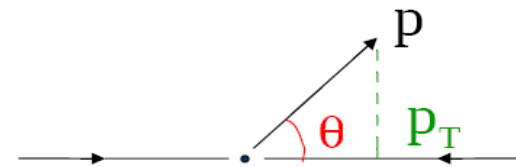


- Length : ~ 46 m
- Radius : ~ 12 m
- Weight : ~ 7000 tons
- $\sim 10^8$ electronic channels
- 3000 km of cables

Transverse momentum

(in the plane perpendicular to the beam)

$$p_T = p \sin\theta$$



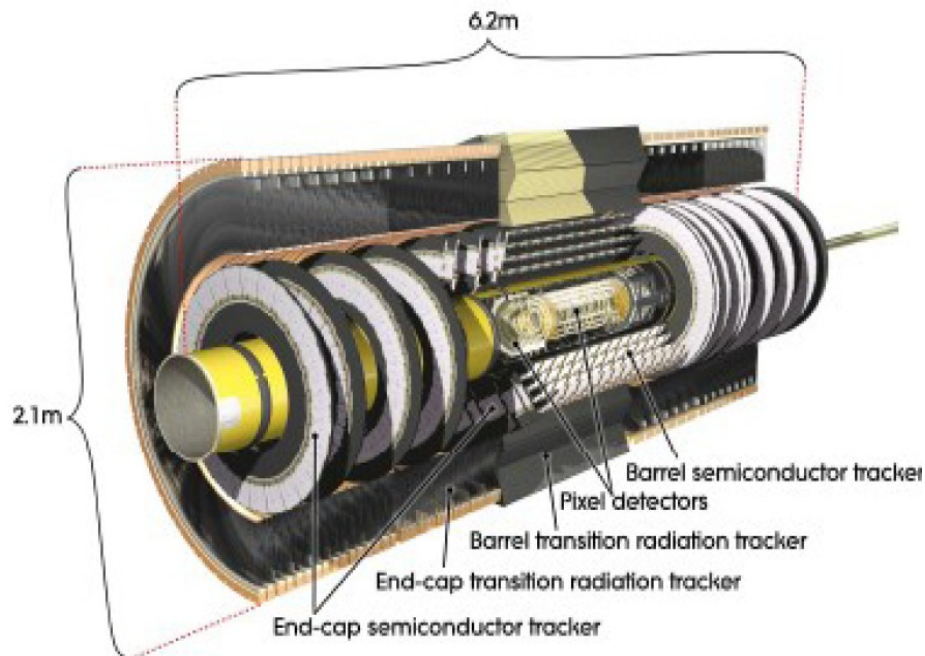
Rapidity: $\eta = -\log(\operatorname{tg} \frac{\theta}{2})$

$$\theta = 90^\circ \rightarrow \eta = 0$$

$$\theta = 10^\circ \rightarrow \eta \cong 2.4$$

$$\theta = 170^\circ \rightarrow \eta \cong -2.4$$

ATLAS Inner Detector



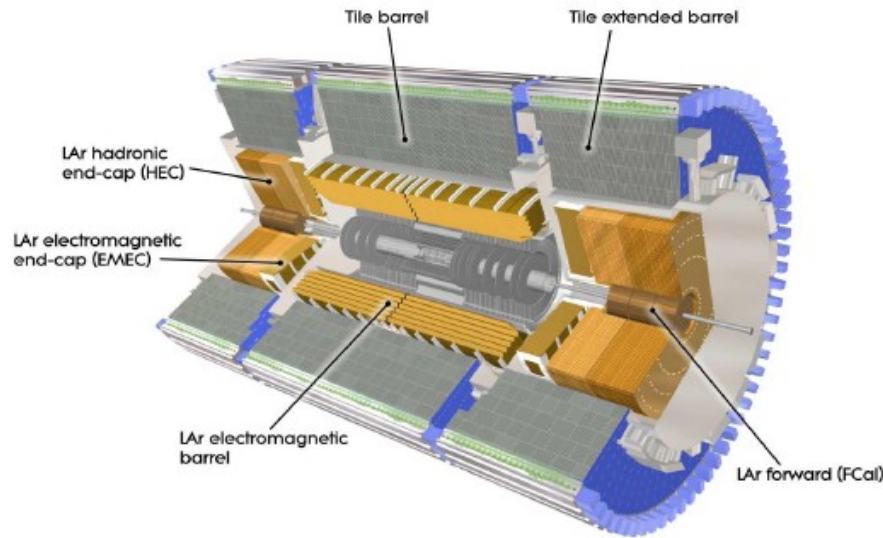
The inner detector $|\eta| < 2.5$ consists of

- Pixel detectors, semi-conductor tracker (SCT), transition radiation tracker

- ≈ 87 million readout channels
- Immersed in 2T solenoidal magnetic field

- Resolution of $\sigma/p_T = 5 \times 10^{-4} \oplus 0.015$

ATLAS Calorimeters



Electromagnetic and hadronic calorimeters

- Subsystem technology and granularity \leftrightarrow shower characteristics
- Transverse and longitudinal sampling \approx 200000 readout cells up to $|\eta| < 4.9$

Electromagnetic Calorimeters:

- Fine granularity
 $\Delta\eta \times \Delta\phi = 0.025 \times 0.025$ in central region
- Energy resolution $10\%/\sqrt{E}$

Hadronic Calorimeters:

- Granularity
 $\Delta\eta \times \Delta\phi = 0.1 \times 0.1$ in central region, less segmented in forward region
- Energy resolution $50\%/\sqrt{E} \oplus 0.03$